



University of South Florida
Scholar Commons

Graduate Theses and Dissertations

Graduate School

3-26-2004

Development Of Cadmium Selenide As An Absorber Layer For Tandem Solar Cells

Sathyaharish Jeedigunta
University of South Florida

Follow this and additional works at: <https://scholarcommons.usf.edu/etd>

 Part of the [American Studies Commons](#)

Scholar Commons Citation

Jeedigunta, Sathyaharish, "Development Of Cadmium Selenide As An Absorber Layer For Tandem Solar Cells" (2004). *Graduate Theses and Dissertations*.
<https://scholarcommons.usf.edu/etd/1093>

This Thesis is brought to you for free and open access by the Graduate School at Scholar Commons. It has been accepted for inclusion in Graduate Theses and Dissertations by an authorized administrator of Scholar Commons. For more information, please contact scholarcommons@usf.edu.

Development Of Cadmium Selenide As An Absorber Layer For Tandem Solar Cells

by

Sathyaharish Jeedigunta

A thesis submitted in partial fulfillment
of the requirements for the degree of
Master of Science in Electrical Engineering
Department of Electrical Engineering
College of Engineering
University of South Florida

Major Professor: Don Morel, Ph.D.
Christos Ferekides, Ph.D.
Y.L.Chiou, Ph.D

Date of Approval:
March 26, 2004

Keywords: css, fill factor, trasmission, substrate temperature

© Copyright 2004 , Sathyaharish Jeedigunta

Dedication

To my parents and brother.

Acknowledgments

I would like to convey my deepest appreciation to my major professor, Dr. Don Morel for giving me an opportunity to be a member of his research group. His excellent guidance was of great help during my thesis work. I am very much thankful for his support and guidance. I would also like to thank Dr. Chris Ferekides and Dr. Y.L. Chiou for their assistance.

I am more than happy to work with my fellow researchers and express my thanks to all of them who have helped me in every stage of my work. My special thanks to Prasanna Mahawela, Harish Sankarnarayanan, Sridevi Vakkalanka, Shirish Pethe, Venkatesh and Madhavi. I am thankful for the encouragement provided by Vijay, Raghu and other friends.

I am thankful to god who has given me his support and blessings. I am very much indebted to my parents and my brother for their encouragement.

Table of Contents

List of Tables	v
List of Figures	vi
List of Abbreviations	ix
Abstract	xii
Chapter 1 Introduction	1
1.1 Introduction	1
1.2 Economics of Photovoltaics	4
1.3 Outline	6
Chapter 2 Background	7
2.1 Photovoltaics	7
2.2 Benefits of Photovoltaics (PV)	7
2.3 Photovoltaic Effect	8
2.4 History	8
2.4.1 Problems with Amorphous Silicon	9
2.4.2 GaAs- an Interesting Material	9
2.4.3 Thin Film Polycrystalline Solar Cells	9

2.4.4 Advantages of Thin Film Polycrystalline Solar Cells	10
2.4.5 Disadvantages of Thin Film Polycrystalline Solar Cells	10
2.5 Structure of Solar Cell	11
2.6 Principle of Operation of Solar Cell	12
2.7 Typical I-V Curve	13
2.7.1 Effect of Series and Shunt Resistance	14
2.7.1.1 Effect of Series Resistance	15
2.7.1.2 Effect of Shunt Resistance	15
2.8 Requirements of the Materials used in Solar Cells	16
2.8.1 Back Contact	16
2.8.2 Absorber Layer	17
2.8.3 Window Layer	17
2.8.4 Front Contact	18
Chapter 3 Literature Review	19
Chapter 4 Device Structure and Fabrication	32
4.1 Tandem Cell Structure	32
4.2 Structure of a CdSe Based Top Cell	34
4.2.1 Substrate	34
4.2.1.1 Cleaning Procedure	34
4.2.2 Back Contact	35
4.2.2.1 Deposition of SnO ₂ : F	36

4.2.2.2 AZO as a Back Contact	36
4.2.2.3 Structure of Cell with AZO at the Back Contact	37
4.2.2.4 Deposition Procedure for AZO	38
4.2.2.5 Transmission of AZO	38
4.2.3 Absorber Layer	39
4.2.3.1 Properties of CdSe	41
4.2.3.2 Preparation of the CdSe Source	41
4.2.3.3 Deposition Procedure for CdSe	41
4.2.3.4 Parameters	42
4.2.3.5 Transmission of CdSe	43
4.2.3.6 Experiments Performed on the Absorber Layer	43
4.2.4 Window Layer	44
4.2.4.1 Properties of ZnSe	45
4.2.4.2 Deposition Procedure for ZnSe	45
4.2.4.3 Evaporation System	46
4.2.4.4 Transmission of ZnSe	47
4.2.5 Front Contact	47
4.2.5.1 Transmission of Copper	48
4.3 Deposition of Cadmium Sulphide	48
4.3.1 Transmission of CdS	50
4.3.2 Structure of Cell with CdSe on CdS/SnO ₂ : F	51

Chapter 5 Results and Discussions	52
5.1 Results	52
5.1.1 AZO as a Back Contact	52
5.1.2 CdS on SnO ₂ : F at the Back Contact	54
5.1.3 Absorber Layer at Higher Substrate Temperatures	57
5.1.4 Effect of Time on Device Performance	63
Chapter 6 Conclusions	66
References	70

List of Tables

Table 3.1 Device Parameters	24
Table 4.1 Properties of CdSe	41
Table 4.2 Properties of ZnSe	45
Table 5.1 Device Parameters for Devices with AZO as a Back Contact	52
Table 5.2 Device Parameters for Devices with CdS on SnO ₂ : F at Back Contact	55
Table 5.3 Effect of Substrate Temperature on Device Performance with 200 Å ZnSe	58
Table 5.4 Effect of Substrate Temperature on Device Performance with 220 Å ZnSe	59
Table 5.5 Effect of Substrate Temperature on Device Performance with 180 Å ZnSe	61
Table 5.6 Effect of Time on Device Performance	63

List of Figures

Fig 1.1 Module World Market Growth	4
Fig 2.1 Substrate Structure	11
Fig 2.2 Superstrate Structure	11
Fig 2.3(a) Equivalent circuit of an ideal solar cell (b) Equivalent circuit of solar cell with series and shunt resistances	12
Fig 2.4 Typical I-V Curve	14
Fig 2.5 Effect of Series Resistance	15
Fig 2.6 Effect of Shunt Resistance	16
Fig 3.1 XRD Pattern of CdSe Film Deposited from an Electrolyte Containing CdCl ₂	20
Fig 3.2 XRD Pattern of CdSe Film Deposited from an Electrolyte Containing CdSO ₄ at a) T=18°C b) T=75°C	21
Fig 3.3 I-V Curve	22
Fig 3.4 Photo-current Action Spectra for Different Electrodes a) OTE/SnO ₂ b) OTE/CdSe c) OTE/SnO ₂ /CdSe	23
Fig 3.5 I-V Curve of CdSe and CdZnSe	25
Fig 3.6 a) AFM results for T _s =300 K b) AFM results for T _s =400 K	26
Fig 3.7 I-V characteristics of a) undoped- PMeT/CBD CdSe b) doped - PMeT/CBD CdSe c) doped - PMeT/CBD CdSe (in presence of Silicon Tungstic Acid)	28
Fig 3.8 Variation of Band gap Vs Deposition Temperature	29
Fig3.9 Variation of Resistivity Vs Deposition Temperature	30
Fig 3.10 J -V characteristics of CdSe thin films with temperature as variable a) with bias voltage < 0.6V b) with bias voltage > 0.6V	31

Fig 4.1 Tandem Solar Cell Structure	32
Fig 4.2 Structure of CdSe Based Top Cell	34
Fig 4.3 Transmission Response of SnO ₂ : F	35
Fig 4.4 Wurtzite Structure of Zinc Oxide	37
Fig 4.5 Structure of Cell with AZO at the Back Contact	37
Fig 4.6 Transmission Response of AZO	38
Fig 4.7 Wurtzite structure of CdSe	39
Fig 4.8 AFM image of CdSe	40
Fig 4.9 Closed Space Sublimation Setup	42
Fig 4.10 Transmission Response of CdSe	43
Fig 4.11 Structure of ZnSe	45
Fig 4.12 Evaporation System	46
Fig 4.13 Transmission Response of ZnSe	47
Fig 4.14 Transmission Response of Copper	48
Fig 4.15 Structure of CdS	49
Fig 4.16 Transmission Response of CdS	50
Fig 4.17 Structure of Cell with CdSe on CdS/SnO ₂ :F	51
Fig 5.1(a) and (b) J-V Curve for Device # sh18-g	53
Fig 5.2 Spectral Response for Device # sh18-g	54
Fig 5.3(a) and (b) J-V Curve for Device # sh39-1-a	55
Fig 5.4 (a) and (b) J-V Curve for Device # sh40-1-e	56
Fig 5.5 Spectral Response for Device # sh39-1-a and # sh40-1-e-a	57
Fig 5.6 J-V Curve for the Devices # sh44-1-f, # sh45-1-e, # sh48-2-1 and sh52-1-1	58

Fig 5.7 (a) and (b) J-V Curve for Devices # sh49-2-f, # sh50-2-e and # sh53-1-1	60
Fig 5.8 (a) and (b) J-V Curve for the Devices # sh49-3-b and # sh51-2-c	61
Fig 5.9 Spectral Response for Devices # sh50-2-e, #sh49-3-b and # sh52-1-f	62
Fig 5.10(a) and (b) J-V Curve for Device # sh44-1-f	64
Fig 5.11 Spectral Response for Device # sh44-1-f	65

List of Abbreviations

eV- electron volt

Q.E-Quantum Efficiency

V_{oc} -Open circuit voltage

I_{sc} -Short circuit current

J_{sc} -Short circuit current density

V_{mp} -Maximum voltage

I_{mp} -Maximum current

R_s -Series Resistance

R_{sh} -Shunt Resistance

I-V-Current-Voltage

PV-Photovoltaic

MW-Mega Watt

A.C-Alternating current

D.C-Direct current

mV-milli volts

mA-milli amps

CIGS-Copper Indium Gallium Diselenide

CdSe-Cadmium Selenide

ZnSe-Zinc Selenide

SnO₂-Tin Oxide
CdS-Cadmium Sulphide
Si-Silicon
GaAs-Gallium Arsenide
AZO-Aluminum doped Zinc Oxide
ITO-Indium Tin Oxide
CdTe-Cadmium Telluride
CdZnTe-Cadmium Zinc Telluride
Mo-Molybdenum
Cu-Copper
HF-Hydro Fluoric
TMT-Tetra Methyl Tin
Cd-Cadmium
ZnO-Zinc Oxide
In-Indium
Al₂O₃-Aluminum Oxide
TCO-Transparent Conducting Oxide
Å -Angstrom
CSS-Close Space Sublimation
CBD-Chemical Bath Deposition
T_{sub}-Substrate Temperature
T_{sou}-Source Temperature
RT-Room Temperature

t_{dep} -Deposition time

$^{\circ}\text{C}$ -Centigrade

α -Absorption coefficient

μ -micron

R-Roughing valve

F-Foreline valve

V-Vent valve

G-Gate valve

Development of Cadmium Selenide as an Absorber Layer for Tandem Solar Cells

SathyaHarish Jeedigunta

ABSTRACT

Cadmium Selenide is a binary compound. It has a band gap of 1.7 eV. This is one of the suitable materials for an absorber layer in the top cell of a tandem solar cell. CIGS with a low Gallium content has a band gap of 1 eV suits well as an absorber layer for the bottom cell. CIGS cells have already attained an efficiency of 15% [1,2]. Since years, research has been done in developing the bottom cell. The results of the bottom cell are promising. So the fabrication of an efficient top cell in a tandem solar cell is a challenge. To achieve a high tandem efficiency of above 25 %, the top cell has to contribute at least 2/3 of the total efficiency, which necessitates the top cell to have at least 16 to 18 % efficiency [3].

Development of a defect free absorber layer is a crucial step in this process to achieve the above goals besides optimizing other layers. Selenium vacancies in CdSe make the absorber layer n-type. CdSe is deposited by closed space sublimation. Deposition of CdSe at higher substrate temperatures in comparison to the standard conditions was studied. ZnSe acts as an insulating layer. It is thermally evaporated in an Evaporation system. Copper acts as a metal contact on top of the insulator resulting in a MIS structure. Copper is also deposited by Thermal Evaporation. Devices are fabricated

on different substrates like SnO₂: F, AZO etc.

Fabricated cells are characterized by J-V and Spectral response measurements. Devices fabricated on SnO₂: F substrates show typical open circuit voltages of around 220 mV, short circuit current densities of 10.02 mA/cm² and fill factors around 33 %. N-type CdS when deposited on SnO₂: F below the absorber layer further improved V_{oc}'s to around 330 mV. Annealing of these devices improved V_{oc}'s to about 350 mV but J_{sc}'s remained 7.21 mA/cm².

Chapter 1

Introduction

1.1 Introduction

As the world's population increases at an alarming rate, the need to meet their requirements is an important aspect to be considered. The modern day computerized world needs less labor. Majority of the tasks are performed by machines driven by power. To perform all these tasks without hindrance, a continuous supply of power is needed.

The conventional sources of energy like hydro, thermal and nuclear are able to meet the current requirements to some extent. But whether the conventional sources of energy are sufficient to meet the demand in coming centuries remains a question. The consumption of non-renewable energies has caused a huge damage to the environment. Electricity generated from fossil fuels has led to high concentrations of harmful gases like carbon monoxide, carbon dioxide, etc in the atmosphere. This in turn led to many problems such as ozone layer depletion and global warming.

Many hydroelectric plants have been constructed in recent past. This is one of the better ways of generating electricity with minimum waste products. Construction of these projects involves a lot of capital to be invested. Moreover most of the rivers are not

perennial and hence cannot generate power continuously through out the year. Another disadvantage of hydroelectric plants is their detrimental effect on the ecosystem. Construction of large hydroelectric plants has caused tremors in those areas.

The nuclear energy is another alternative source of energy, which has a potential to produce many megawatts of power. Nuclear energy if used for constructive purposes can generate power. On the other hand if it is used for destructive purposes can be benignant to human life. The option of nuclear energy raises safety issues like disposal of its waste products. So these factors make many nations to rethink about constructing nuclear plants.

Hence an alternative form of energy is an obvious choice to meet the requirements. Thus there is an immediate need for the development of non-conventional energy sources. Tidal, solar, geo-thermal and wind are few non-conventional energy sources. These are inexhaustible energy sources and hence are renewable. They cause fewer emissions. Their use can reduce pollution. They stand out as a viable source of clean and limitless energy.

The tidal energy would be an attractive alternative if it were more reliable. However the vast regions across the world are covered by land and hence it is not a feasible option. Windmills do not meet the practical applications of present day. They can be used only for some specific purpose and also cannot generate many megawatts of power.

Sun is the center of all the activities in the world. It is calculated that in every second about 6×10^{11} kg of H_2 is converted to He in sun. An enormous amount of energy (approx 4×10^{20} J) is produced in this process [9]. This energy is emitted as an electromagnetic radiation. It is projected that this constant amount of energy can be obtained for at least 10^{10} years. Hence among the above renewable energy sources, solar energy is the most readily available source of energy.

But how can we tap this bountiful source of energy? Research in this field has led to the development of first photo-voltaic cell (Bell laboratories, 1954) [4]. In 1960's, photo voltaic modules were used to power space satellites. Since then many researchers have spent decades in this field in making solar energy a viable alternative.

The first homojunction silicon solar cell developed during 1954 had an efficiency of only 6 %. But the progress in silicon technology resulted in single crystal silicon solar cells with high reliability and efficiencies reaching above 25 %. These silicon photo-voltaic modules are very expensive. Less expensive polycrystalline silicon modules surpass the previous ones. Polycrystalline materials result in less efficient solar cells than single crystal silicon. Currently about 95 % of commercially available photovoltaic modules are made from crystalline silicon cells and only 5 % is contributed by thin film technology [5]. Thin films solar cells have become a very good competitor for the single crystal and polycrystalline silicon solar cells because of their cheaper raw material as well as processing costs. Substrates used in thin film solar cells are either a metal or a glass or a polymer. These are relatively cheaper when compared to silicon wafers.

1.2 Economics of Photovoltaics

The average cost per kilowatt-hour from conventional energy sources is 6-7 cents [6]. Present day photo-voltaics generate 20-30 cents per kilo watt-hour. Hence the cost per kilo watt hour should be reduced by 4 to 5 times to make PV an economical candidate.

Various factors like module efficiency, lifetime and cost per unit area effects the PV energy cost. Lower efficiency module costs less than an equivalent higher efficiency module to produce the same amount of electricity.

According to the statistics of 2001, PV market is generating 381 MW of power which is being divided among US, Japan and few European nations. U.S companies export 75 % of PV products to developing countries. Market growth in last decade was about 15 - 25 %. Market growth will depend on the continuing decline of PV costs relative to conventional supplies.



Fig 1.1 Module World Market Growth

Support programs in many countries are involved in accelerating the market growth. In Germany, a law was passed which sets a rebate rate of 0.5 Euro/Kwh of PV generated electricity. Japan's very ambitious 70,000 roof program resulted in 63 % of its production in 1999. Interest in this roof top application started in USA during 1970's [7]. Japan also came into the race in mid 1980's with the construction of a test bed for over 200 residential systems on Rokko Island in 1986. After several years of evaluating technical issues to their grid connection, a subsidized installation program was launched by the Japanese government in 1993. By 2010 Japan targets to meet a 1.5 million rooftop applications.

US government announced a "million roof" program in mid 1997 targeting this number of systems by 2010. At the end of 1997, European Union also agreed to a similar target by 2010 with half the systems to be installed in Europe and half outside. Since then other countries like Netherlands, Italy and Australia have announced targets for photovoltaic roofs.

The demand for electricity is often highest during the day. Solar energy can be drawn more in those parts of world near the equator. Other economical issue that has to be taken into consideration is the installation of inverters to get an A.C output. The grid also requires battery setup for the energy to be stored so that it can be used whenever it is required.

1.3 Outline

After having discussed about the various kinds of energy sources-conventional and non-conventional, silicon cells, economics of photovoltaics, further topics stress on background, history of photovoltaics, solar cells. A review on literature helps readers to better understand the ongoing research. Major focus is on experiments performed and on results obtained. A few conclusions are drawn with some suggestions towards achieving the future goals.

Chapter 2

Background

2.1 Photovoltaics

Photovoltaics (PV) is the direct conversion of sunlight to electricity. When photons of energy greater than the band gap are incident on a semiconductor, electrons are excited from valence band to the conduction band. If these excited electrons can be collected before they recombine, electricity can be produced. Electricity obtained can be used right away, can be converted to AC or can be stored for a later use. PV systems are modular and hence they can be engineered for any size of application from a smallest wrist watch to a huge power station.

2.2 Benefits of Photovoltaics (PV)

PV has many benefits. A few of them are:

Reliability: Photovoltaics operate reliably for long periods of time without any maintenance.

Low costs: They have low operating costs.

Environment friendly: They are pollution free and have no by products or wastes. They are clean and silent.

Secure energy: Photovoltaics provide inexhaustible domestic energy.

2.3 Photovoltaic Effect

The technique of conversion of solar energy to electricity occurs by “photovoltaic effect” which was first observed by Antoine Ceaser Becquerel in 1839[8].It is defined as “an emergence of an electric voltage between two electrodes attached to a solid or liquid system upon shining light on to this system”.

2.4 History

Few decades after the discovery of photovoltaic effect, a group of scientists observed that solid selenium also exhibited photo conductivity when light was incident on it. Initially the research was focused on selenium and cuprous oxide cells. But they did not show any promising performance .They had efficiencies of around 1 %. Nearly after four decades of no significant progress, people started to explore new materials for photovoltaic applications. During 1954 three scientists, Chapin, Fuller and Pearson were successful in developing a homojunction silicon solar cell with an efficiency of 6 % [9]. Further research resulted in attaining efficiencies of around 10 %.Silicon solar cells found their first commercial application in space crafts. The first silicon solar cells were made from single crystal silicon. The manufacturing process of single crystal silicon from its raw material involves various intermediate steps making single crystal silicon expensive. Single crystal silicon is an indirect band gap semiconductor and hence it requires more material to absorb light.

During the same period polycrystalline Si, amorphous silicon, GaAs and thin film solar cells like $\text{Cu}_x\text{S}/\text{CdS}$ were developed. $\text{Cu}_x\text{S}/\text{CdS}$ solar cells had an efficiency of 6 %.

Further progress improved their efficiency to 9 %.But these cells degraded because of copper diffusion.

2.4.1 Problems with Amorphous Silicon

Amorphous silicon is another viable candidate as a solar cell material. But these cells showed comparatively lesser efficiencies. This could be because the crystal structure of the material. Amorphous silicon solar cells performed poorly when compared to its counterparts because of their instability. Their performance degraded considerably over a period of time.

2.4.2 GaAs- an Interesting Material

The emerging technologies aim at bringing an optimization between the performance of cells and their processing costs. GaAs is a direct band gap material with a band gap of 1.43 eV. During 1970's reasonable efficiencies of around 10 % were reported for GaAs cells. Solar cells with GaAs are expensive due to high material and processing costs. Therefore a wide range of promising polycrystalline compound semiconductor materials become a choice in solar cell processing.

2.4.3 Thin Film Polycrystalline Solar Cells

Polycrystalline materials are composed of many localized single crystals. These single crystals are called grains. The transition regions in polycrystalline solids existing between various single crystals are called grain boundaries. These regions contain structural and bonding defects which act as centers for impurity collection.

Most of the thin film polycrystalline semiconductor materials have a direct band gap. Hence it is easy to excite electrons from the valence band to the conduction band. Most of these materials have high absorption coefficients so that few micron thick film is enough to absorb major portion of the solar spectrum. The range of operating temperatures is less and hence more uniform polycrystalline films can be obtained. It also involves inexpensive processing techniques and material costs.

2.4.4 Advantages of Thin Film Polycrystalline Solar Cells

- a) Low processing costs.
- b) Relatively less material costs.
- c) Substrates used mostly are glass, metal sheet or polymers which are inexpensive.
- d) Thin film solar cells can be produced on large area substrates giving a high output with a low unit cost.

2.4.5 Disadvantages of Thin Film Polycrystalline Solar Cells

- a) Thin film polycrystalline solar cells have lesser efficiencies when compared to its equivalent counter parts.
- b) Polycrystalline materials have grain boundaries. They have crystal defects. These defects are the centers of impurities. These defects act as recombination centers. Recombination of charge carriers result in poorer electronic properties.
- c) Reproducibility of large area uniform films is not assured.
- d) Stability of these cells is another issue to be yet resolved.

2.5 Structure of Solar Cell

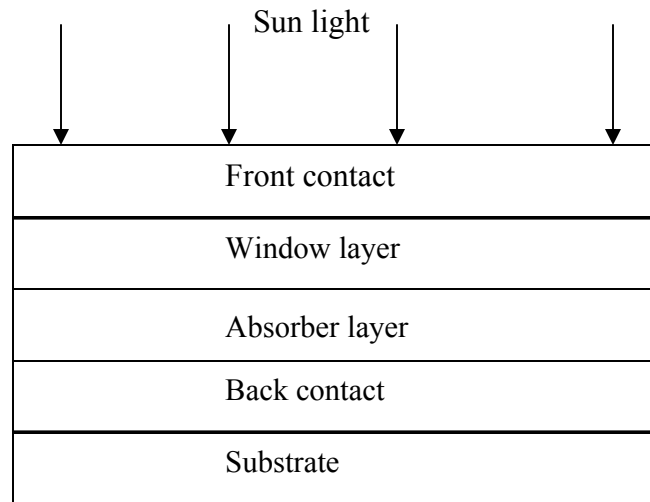


Fig 2.1 Substrate Structure

A solar cell can have two structures, superstrate structure or a substrate structure. The difference between these two structures is that in a substrate structure light is incident at the front contact whereas in a superstrate structure light first passes through the substrate. The two structures are shown in Fig 2.1 and Fig 2.2 respectively. For a tandem solar cell these two structures are placed one over the other so that the top cell absorbs the lower wavelengths and the bottom cell absorbs the higher wavelengths.

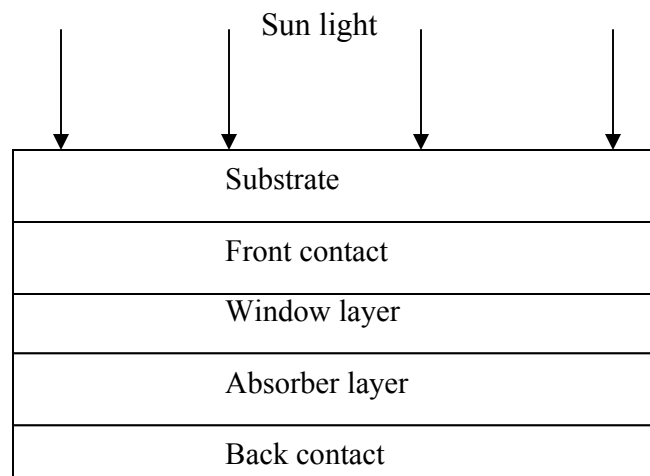


Fig 2.2 Superstrate Structure

2.6 Principle of Operation of Solar Cell

A solar cell is a p-n junction. Solar energy is converted into electricity when light is incident at the junction. When light is incident at the junction, photons with energy lesser than the bandgap makes no contribution to the output. Photons with energy greater than the bandgap will contribute energy equal to the bandgap to the output while the excess energy will be wasted as heat. The absorbed energy generates charge carriers across the junction which can be separated by the electric field present at the junction. Equivalent circuit of an ideal solar cell is shown in Fig 2.3 (a). An equivalent circuit of the solar cell with the losses due to series and the shunt resistances is shown in Fig 2.3 (b).

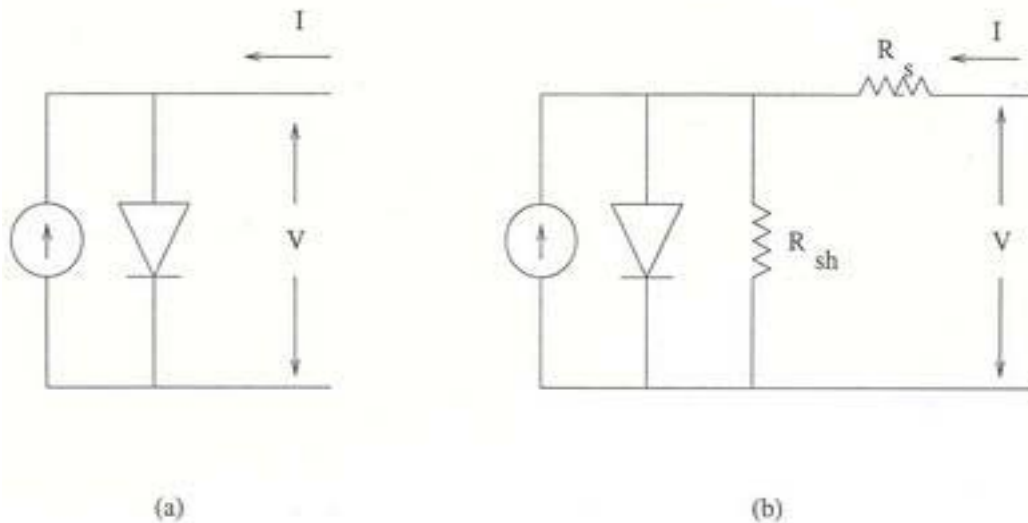


Fig 2.3(a) Equivalent circuit of an ideal solar cell (b) Equivalent circuit of solar cell with series and shunt resistances

Under no illumination, current across the junction is given by the ideal diode equation

$$I=I_0[(e^{qV/AKT}-1)] \quad (2.1)$$

Under illumination due to the generation of charge carriers, a current I_L flows through the junction. The current across the junction is given by eq(2.2)

$$I=I_0[(e^{qV/AKT}-1)]-I_L \quad (2.2)$$

Where I_0 is the reverse saturation current

I_L is the light generated current

A is the diode ideality factor

2.7 Typical I-V Curve

A typical I-V response of a solar cell is shown in Fig 2.4[8]. In eq (2.2) when current I is made zero, V_{oc} is given by

$$V_{oc} = (AKT/q)*[\ln (I_L/I_0 +1)] \quad (2.3)$$

Similarly under short-circuit conditions, when voltage V is zero in eq(2.2) the short circuit current is given by

$$I_{sc} =-I_L \quad (2.4)$$

V_{mp} and I_{mp} are the maximum voltage and current that can be extracted at the output. The squareness of the curve determines the output parameters of a device.

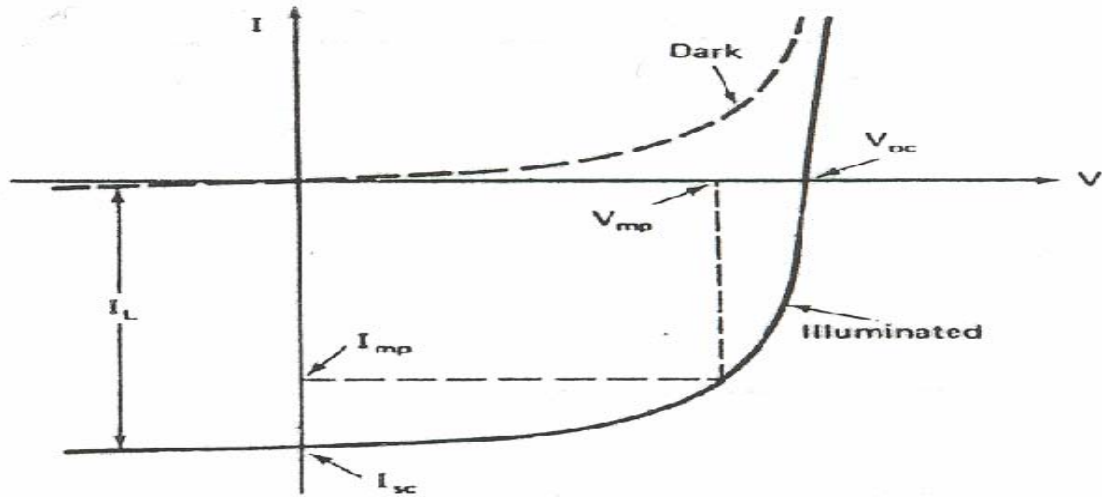


Fig 2.4 Typical I-V Curve

The maximum power from a solar cell is given by

$$P_{mp} = I_{mp} * V_{mp} \quad (2.5)$$

The efficiency of a cell is given by

$$\eta = P_{mp} / P_{in} \quad (2.6)$$

$$\eta = I_{mp} * V_{mp} / P_{in} \quad (2.7)$$

$$\eta = I_{sc} * V_{oc} * FF / P_{in} \quad (2.8)$$

$$FF = I_{mp} * V_{mp} / I_{sc} * V_{oc} \quad (2.9)$$

P_{in} is the incident power.

FF is the Fill factor.

2.7.1 Effect of Series and Shunt Resistance

A practical solar cell has losses due to both series and shunt resistance. The practical diode equation including the series and shunt resistance is given by

$$\ln\left(\frac{I + I_L}{I_S} - \left(\frac{V - IR_S}{I_S R_{SH}}\right) + 1\right) = (q/kT) * (V - IR_S) \quad (2.10)$$

2.7.1.1 Effect of Series Resistance

The series resistance is mainly due to ohmic losses and resistance of the bulk semiconductor. The effect of series resistance on the I-V curve is shown in Fig 2.5.

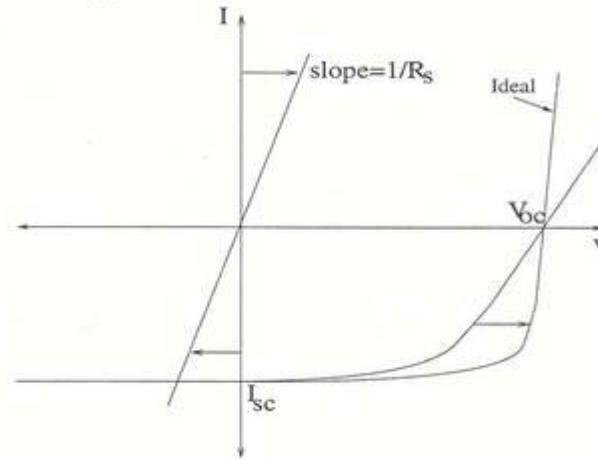


Fig 2.5 Effect of Series Resistance

The series resistance for a practical cell should be in the order of tenths of ohms.

When $R_{SH} = \infty$ and V is Zero eq(2.10) can be written as

$$\ln\left(\frac{I+I_L}{I_S}+1\right) = \frac{q}{kT}(-IR_S)$$

Therefore $I = I_S \exp\left(-\frac{qIR_S}{kT}\right) - I_L$

Hence the increase in the series resistance results in lesser short circuit currents.

2.7.1.2 Effect of Shunt Resistance

The Shunt resistance is due to leakage currents. This results in high reverse saturation currents. From eq(2.3) higher value of I_0 result in lower V_{oc} 's. Hence the effect of shunt resistance is reduced V_{oc} 's. The effect of shunt resistance on I-V characteristics is shown in Fig 2.6.

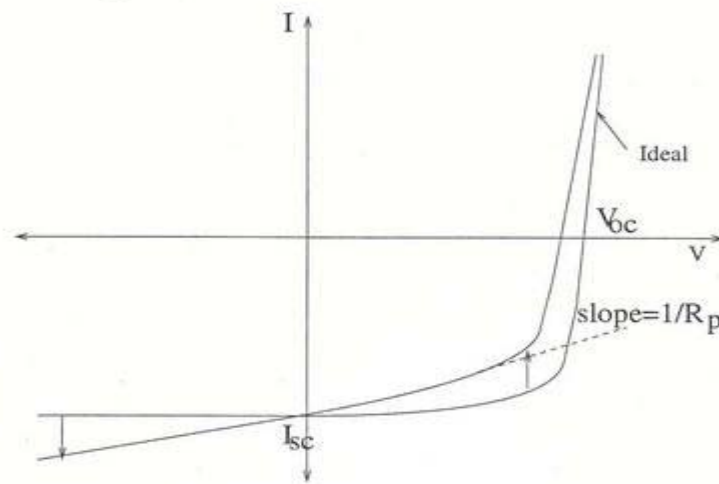


Fig 2.6 Effect of Shunt Resistance

2.8 Requirements of the Materials used in Solar Cells

Semiconductor materials used to fabricate solar cells should be sensitive to the color of light. Certain materials absorb more light and while others absorb less. The amount of absorption depends on the absorption coefficients of the materials. The materials used should have good optical properties so that optical losses due to reflection, scattering can be reduced. The requirements of materials used in different layers of the solar cells are discussed below.

2.8.1 Back Contact

A back contact should have low resistivity and be able to form a good ohmic contact to the absorber layer. It should have high mechanical stability and must have good adhesion to the substrate. SnO_2 : F, AZO (Al doped ZnO), ITO (Indium Tin oxide) are few TCO's. SnO_2 : F is mainly used as a back contact in this work.

2.8.2 Absorber Layer

The absorber material should have a direct band gap so that light can be absorbed efficiently. Thickness of the absorber layer depends on the absorption coefficients of the material. Bandgap of the absorber determines the output voltage of the cell. Higher bandgap results in higher output voltage but lower short circuit currents and viceversa. Materials used as absorbers should have high minority carrier lifetimes so that they can be collected before they recombine. Defect free absorber layer is required for a good performance of solar cell. It should have a good lattice match with the window layer.

A large variety of inorganic, organic, crystalline, polycrystalline and amorphous materials can be used as an absorber layer [10]. During 1980's CdSe has drawn lot of interest of many researchers as a photo-electrochemical cell [11]. But the efficiency obtained was only 6 % [12]. CdSe is a binary compound with a direct band gap of 1.7 eV. It has a high absorption coefficient of 10^4cm^{-1} . CdSe has a lattice constant of 6.05 Å.

2.8.3 Window Layer

A window layer should have a large band gap with minimum absorption and maximum transmittance. The ideal bandgap of a material to be used as a window layer should be greater than 2.5 eV so that it can transmit maximum amount of light to the absorber. There should be good lattice match between the window and the absorber layer materials.

ZnSe has a band gap of 2.7 eV. It has 90 % transmission in visible region. It has a lattice constant of 5.66 Å. The lattice mismatch between CdSe and ZnSe is around 6.5%.

2.8.4 Front Contact

A Front contact should have low reflectance and high transmittance. It must have low resistivity and be able to form a good ohmic contact with the window layer. Copper is deposited as a front contact in all the devices.

Chapter 3

Literature Review

Most of the II-VI compounds have drawn interests of many people in research because they find their applications in optoelectronic devices, photo electrochemical cells, thin film transistors [23], gas sensors [24, 25], acousto-optical devices [26], vidicones [27], photographic photoreceptors [28] and gamma ray detectors.

Among II-VI compounds CdTe, HgI₂, CdS, CdSe etc are prominent because of their properties like direct band gap, high absorption coefficients etc. CdTe, CdS and CdSe find its applications in photovoltaic devices and HgI₂ finds its application in detectors. Different techniques have been used in depositing these materials and in fabricating devices. Close Space Sublimation (CSS), Chemical Bath deposition (CBD), Sputtering, Thermal Evaporation, Molecular Beam Epitaxy (MBE) and Metal Organic molecular beam epitaxy (MOMBE) are some of the vacuum deposition techniques. Lot of research has been done in past years and literature reflects the progress made in this field. In this section, a brief review of literature on CdSe for optoelectronic applications done by various research groups is mentioned.

E. Benamar [13] et al employed a method called “cathodic electrodeposition” for depositing polycrystalline CdSe films on ITO/glass substrates. Electrocodeposition is a low cost technique which can be used effectively for large area films. The process involved a potentiostatic reduction of CdSe from acid aqueous bath. The aqueous solution had 0.2 M CdSO₄ (Cadmium sulphate) or CdCl₂ (Cadmium chloride) and 7 X 10⁻⁴ M H₂SeO₃ (Selenious acid) for simultaneous codeposition of Cd and Se ions. The process involved the reduction of Cd ions and Se ions at the cathode thereby depositing a film on the substrate. They claim that when CdSO₄ is used as a source for Cd ions, CdSe deposited had cubic structure. By using CdCl₂ both cubic and hexagonal forms of CdSe was observed.

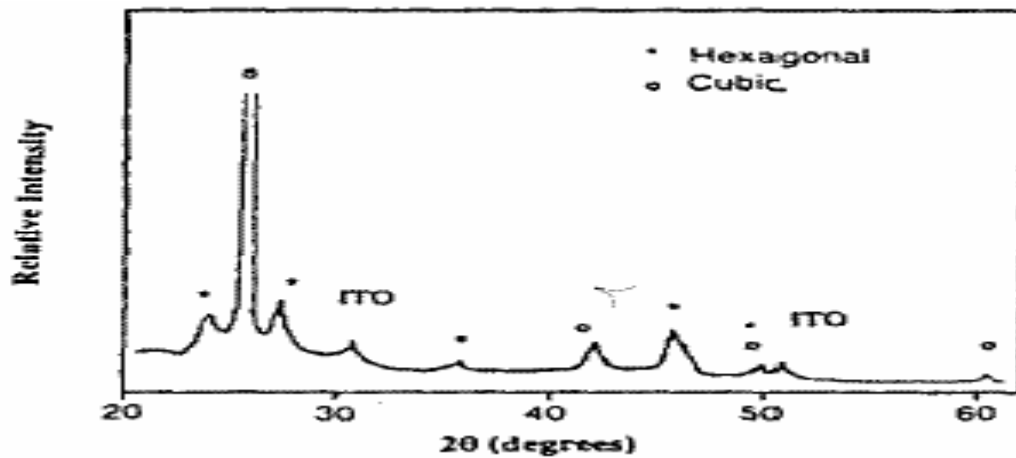


Fig 3.1 XRD Pattern of CdSe Film Deposited From an Electrolyte Containing CdCl₂

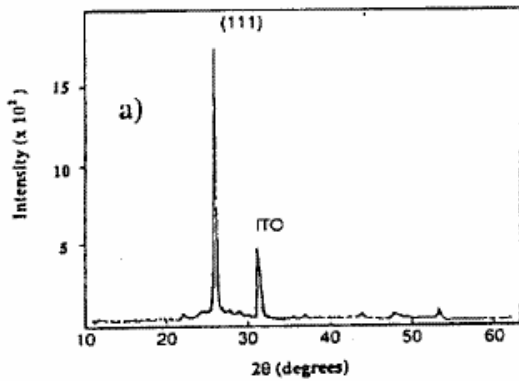


Fig 3.2(a)

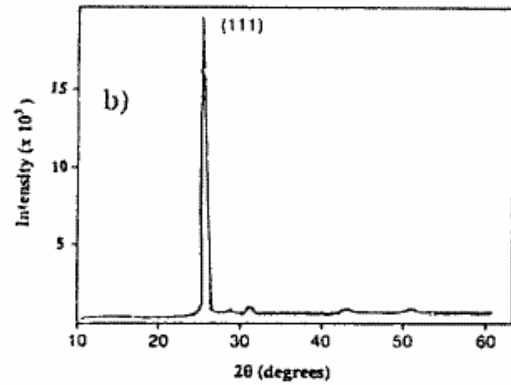


Fig 3.2(b)

Fig 3.2 XRD Pattern of CdSe Film Deposited from an Electrolyte Containing CdSO₄ at a) T=18°C b) T=75°C

Using CdSO₄ as an electrolyte, CdSe was deposited on ITO substrates at 18° C and 75° C. From Fig 3.2(a) it can be observed that the peak at an angle of $2\theta = 30^\circ$ flattens when the temperature was increased from 18° C to 75° C. In Fig 3.2(a) and (b) CdSe films on ITO substrates grow with a preferential orientation of (111). SEM studies showed that modular spanning of 1- 4 μ m or less in extent is present.

From Fig 3.3 they have obtained the values of V_{oc} as -0.7V and I_{sc} as 1.7mA. A FF of 0.49 % and an efficiency of 1 % is obtained. They attributed the results to the kinetic properties of the interface.

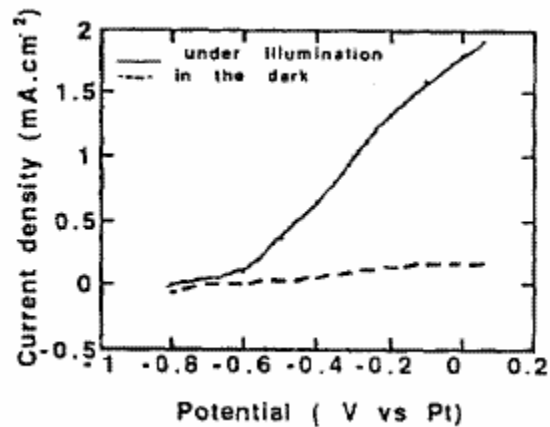


Fig 3.3 I-V Curve

Another group lead by Chouhaid Nasr [14] et al at Radiation laboratory, University of Notre Dome conducted comparative studies on photoelectrochemical behavior of SnO₂/CdSe and OTE/SnO₂/CdSe nanocrystalline films. ITO coated glass was used as an optically transparent electrode (OTE).SnO₂ was coated on OTE and was dried in air on a hot plate. The films were then annealed for 1 hour at 673 K. CdSe films were deposited both on OTE and OTE/SnO₂ .CdSO₄ and SeO₂ (Selenium dioxide) were chemicals used in the reaction .They conducted both electrical and optical measurements which suggested that coupling of OTE/SnO₂/CdSe had better performance when compared to SnO₂/CdSe in terms of conversion efficiency and stability.OTE/SnO₂ electrode absorbed light below 400 nm whereas OTE/SnO₂/CdSe absorbed till 700 nm with a peak value at 470 nm.

In a nanocrystalline film, there was no space charge region and hence the charge separation took place by the kinetics of reactions. Tests conducted proved that the charge separation process was more effective in a coupled system (OTE/SnO₂/CdSe). In a

coupled system photogenerated electrons migrate to the conduction band of SnO₂ and hence prevent recombination with holes present in CdSe film. But when CdSe was deposited directly on OTE there was more recombination taking place before the carriers could reach the back contact. Hence it drops the photo current by a large magnitude.

Fig 3.4 compares the photo-current action spectra of different electrodes. Typical cells showed a V_{oc} and a J_{sc} of 0.550V and 27μAcm⁻² respectively. FF was 0.47. An efficiency of 2.25 % was achieved for an incident power of 0.3mWcm⁻². They concluded that coupling of CdSe and SnO₂ improved the performance of OTE/SnO₂/CdSe rather than SnO₂/CdSe alone.

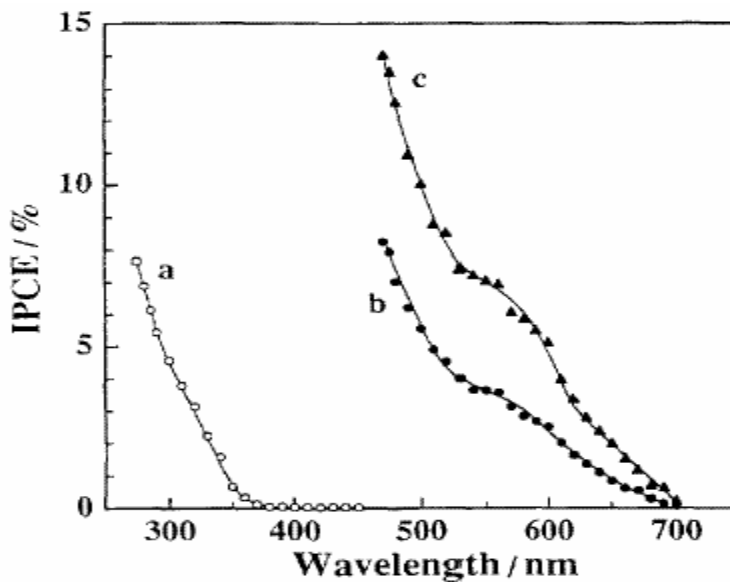


Fig 3.4 Photo-current Action Spectra for Different Electrodes a) OTE/SnO₂ b) OTE/CdSe c) OTE/SnO₂/CdSe

Meera Ramarahiani [15] studied the characteristics of Zinc doped polycrystalline CdSe films. CdSe films were first deposited on Titanium substrates at room

temperature from a solution of SeO_2 , CdSO_4 and H_2SO_4 by a process called electrocodeposition. These films were then annealed at 400°C for 2.5 hrs. Zn ions were then incorporated on CdSe by dipping the film in an aqueous solution of ZnSO_4 . This was followed by heating in air at 100°C for half an hour. Incorporation of Zn ions at the surface produced favorable states in the band gap which improved the charge transfer kinetics at the interface thereby reducing the recombination process. Upon heating these films, Zn diffused through the grain boundaries and reduced the recombination centers for majority carriers. When some of the Cd atoms were replaced by Zn atoms, the bandgap of the material increased. Hence V_{oc} was improved but I_{sc} was reduced to some extent. This could be because of the formation of $\text{Cd}_{1-x}\text{Zn}_x\text{Se}$. $\text{Cd}_{1-x}\text{Zn}_x\text{Se}$ has a bandgap lying between the bandgaps of both CdSe and ZnSe. This material with a higher bandgap than CdSe contributes to the increase in V_{oc} . Photoelectrode was prepared by applying a common epoxy. Copper leads were spot welded at the back contact for electrical connections. Deposition time was optimized to be 45 min and a film of approximately $4\ \mu\text{m}$ was grown on Titanium substrate. Following are the parameters of a typical device.

Table 3.1 Device Parameters

	$V_{oc}(\text{mV})$	$I_{sc}(\mu\text{A})$	$P_{MAX}(\text{Nw})$	FF
CdSe	42.5	16.2	214	0.33
$\text{Cd}_{1-x}\text{Zn}_x\text{Se}$	53.5	20.8	497	0.45

I-V characteristics are shown in Fig 3.5. They claimed that I-V characteristics of Zn incorporated CdSe film showed a positive shift and concluded that doping of Zn on the surface of n-CdSe films improved the performance.

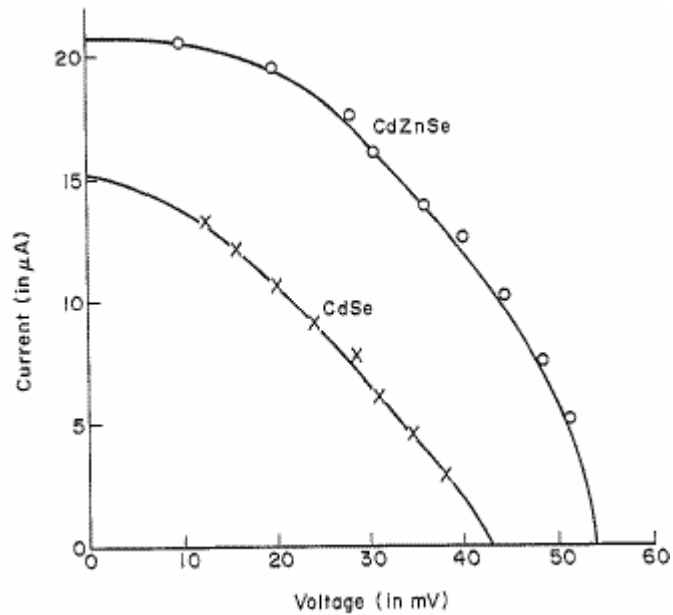


Fig 3.5 I-V Curve of CdSe and CdZnSe

Cristian Baban et al [16] studied the structural and optical characteristics of thermally evaporated CdSe thin films on glass substrates. The influence of preparation conditions on the fundamental absorption of CdSe thin films was also studied. Polycrystalline powder of CdSe was thermally evaporated by a quasi- closed volume technique. Thin film samples were deposited at various source and substrate temperatures. XRD studies revealed that the films had a hexagonal wurtzite structure with (002) orientation. AFM tests confirmed that the grain size was between 20 - 100 nm (shown in Fig 3.6). They concluded that as source and substrate temperature increases, crystal size also increases.

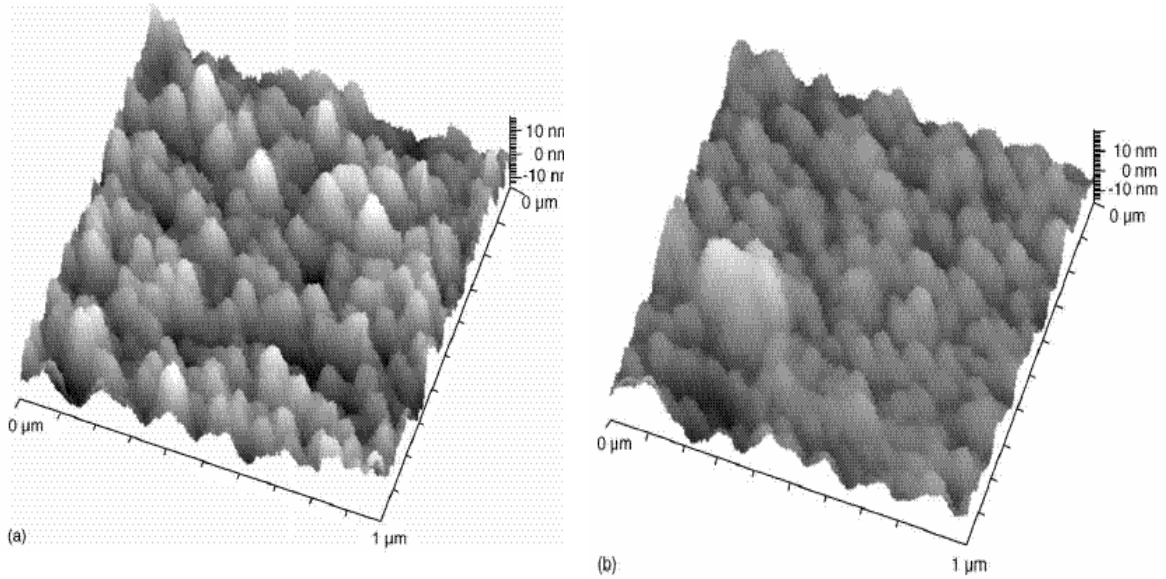


Fig 3.6 AFM results for a) $T_s=300$ K

b) AFM results for $T_s=400$ K

The films were annealed at 200°C for 30 minutes after deposition. Annealed samples showed an increase in crystal size. The transmission response of both annealed and as deposited samples was observed. They concluded that as deposited samples had lesser transmission when compared to annealed ones. They attributed this to the increase in the crystal size. This might be because as the crystal size increases, the number of grain boundaries decrease resulting in the decrease of scattering effects thereby improving the transmission.

D.Pahinettam Padiyan et al [17] observed the influence of thickness and substrate temperature on electrical and photoelectrical properties of vacuum deposited CdSe films on glass substrates. Optical studies of the films confirmed that the band gap decreases with an increase in the thickness of the films and substrate temperature. CdSe powder with 99.99 % purity was taken as a source material. The films were deposited at three

different temperatures- Room temperature (RT), 100°C and 200°C. As claimed in the previous paper, this group also stated that the grain size increased with an increase in the substrate temperature. The band gap energies at different temperatures were observed to vary and they attributed this to the grain size. By conducting photoelectrical measurements, they concluded that the dark and light currents for as deposited substrates increased with an increase in the film thickness and substrate temperature.

C.Sene et al [18] studied the effects of silicotungstic acid on CdSe films grown on polymer substrates. They employed CBD for depositing films on various substrates like glass, gold, ITO and an organic polymer material (PMeT (poly (3-methylthiophene))). This polymer was either a p-type or a quasi metallic conductor. The focus was on organic - inorganic photovoltaic junctions. CdSe deposited by CBD on PMeT formed a p-n junction. Electropolymerization of CBD CdSe formed a Schottky-type junction. P-N junction obtained a conversion efficiency of 0.03 % while the Schottky-type junction had a conversion efficiency of 1.3 %. The presence of silicotungstic acid in the chemical bath increased the conversion efficiency of Schottky-type junction to 2.7 %. The optical and structural properties of CdSe film depended on the type of substrate that was used. Photovoltaic properties of CdSe/doped PMeT and CdSe/ undoped PMeT junctions were studied. They stated that the use of silicotungstic acid resulted in forming highly efficient junctions.

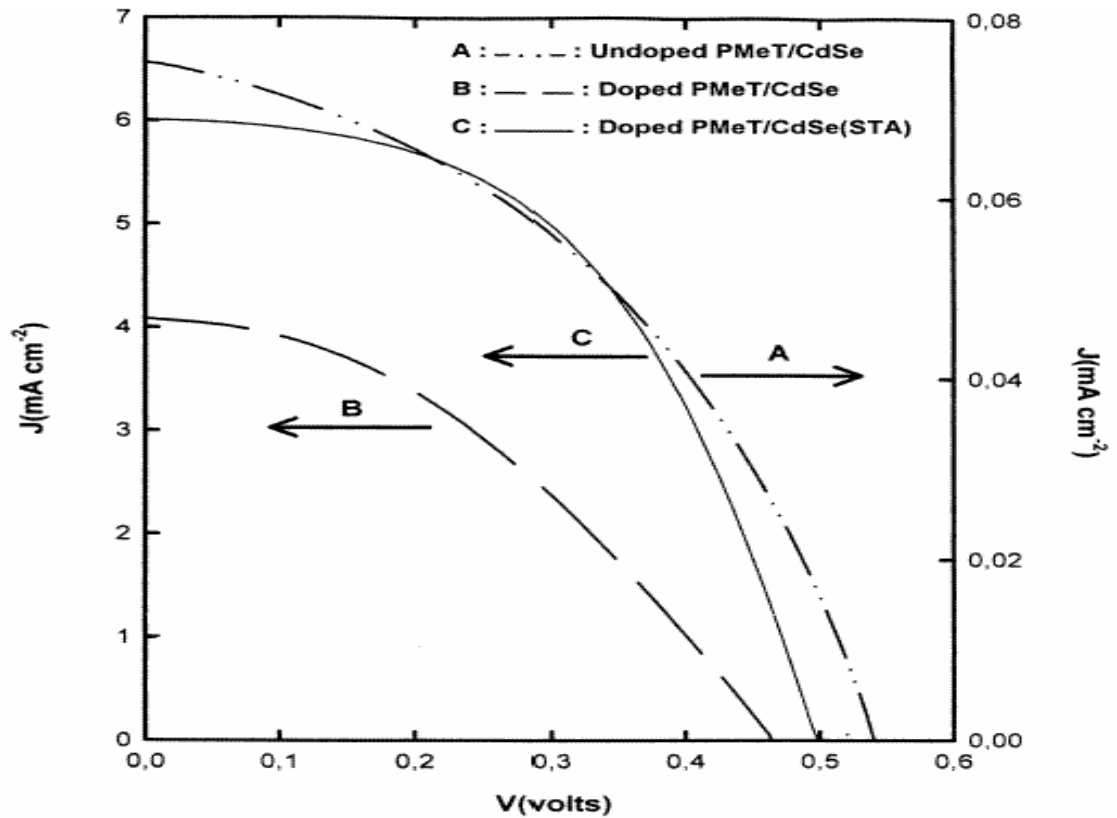


Fig 3.7 I-V characteristics of a) undoped- PMeT/CBD CdSe b) doped - PMeT/CBD CdSe c) doped - PMeT/CBD CdSe (in presence of Silicon Tungstic Acid)

From Fig 3.7 it can be observed that undoped PMeT/CBD CdSe junction has obtained higher voltage. Doped PMeT/CBD CdSe has resulted higher current density when compared to undoped PMeT/ CBD CdSe while doped PMeT/CBD CdSe in presence of Silicon tungstic acid has resulted in a higher current density than the other two junctions.

S.S.Kale et al [19] studied the thickness dependent properties of CdSe thin films deposited by chemical deposition method. The effect of thickness on electrical, structural and optical properties was studied. The chemicals used in the process were 0.1 M CdSO₄ solution, 0.13 M Na₂SeSO₃ (Sodium Selenite) solution and Ammonia. The

deposition temperature was varied between 273 K and 358 K and the corresponding thicknesses of films were measured to be between 600 Å and 2400 Å respectively.

They concluded that as the deposition temperature decreased from 358 K to 273 K, thickness decreased from 2400 Å to 600 Å and grain size decreased from 80 to 40 Å. As the temperature was increased, disassociation of the complex and the anion, the rate of release of selenium and thickness of the films increased. Larger grains were obtained. From Fig 3.8 it can be noticed that there is a linear variation of band gap with the deposition temperature. Band gap increased from 1.90 to 2.4 eV as the deposition temperature was decreased from 358 K to 273 K. They attributed this to quantum size effect.

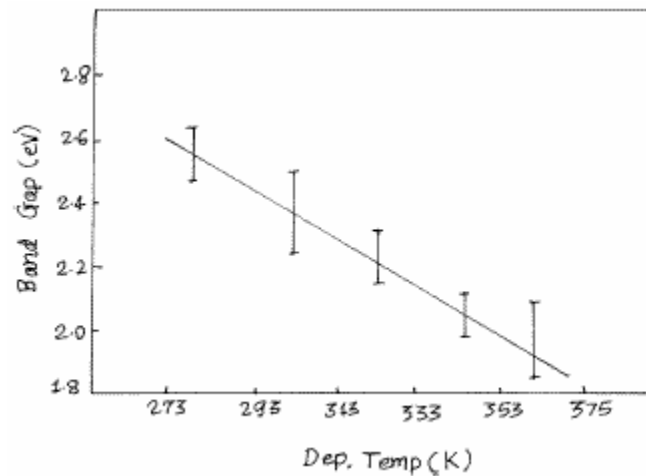


Fig 3.8 Variation of Band gap Vs Deposition Temperature

When the electrical properties were studied they observed that the resistivity increased from 10^3 to 10^4 Ω cm as the deposition temperature decreased from 358 K to 273 K. In general the resistivity of a nanocrystalline material is more than a

polycrystalline material. Hence the high resistivity at low deposition temperatures could be because of its smaller grain size. The variation in resistivity with deposition temperatures is shown below.

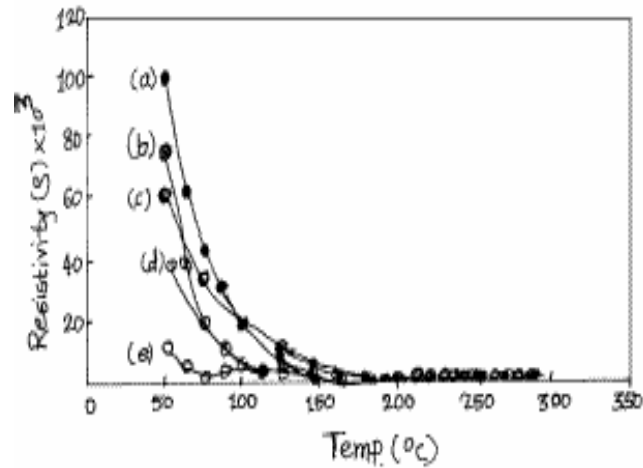


Fig 3.9 Variation of Resistivity Vs Deposition Temperature

R.M.Abdel-Latif at University of Minia [20], Egypt studied about the electrical properties of evaporated CdSe thin films. Aluminum with high purity (99.99%) was evaporated from a tungsten filament onto a cleaned glass substrate through a mask to form a base electrode. Pure CdSe was deposited through a mask from a molybdenum boat. A top electrode of Au was deposited over this. The substrate was maintained at room temperature.

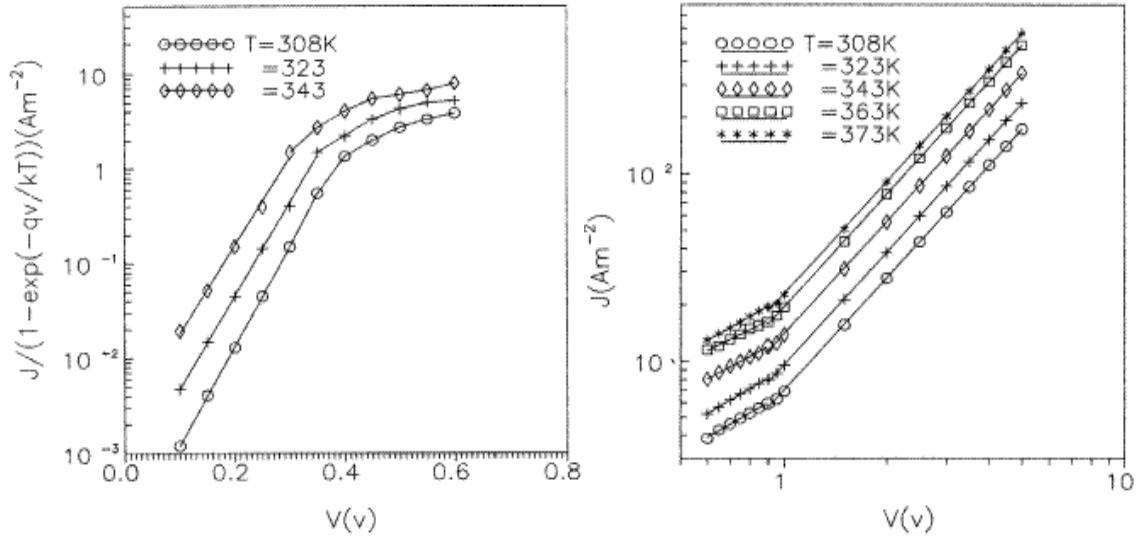


Fig 3.10 J -V characteristics of CdSe thin films with temperature as variable a) with bias voltage < 0.6V b) with bias voltage > 0.6V

The J-V characteristics of the devices are shown in Fig 3.10. As the deposition temperature was increased, there is an increase in the variation of the current density with the voltage. They have concluded that for Al-CdSe-Au thin films at low voltages, current varies exponentially with voltage. They have further stated that the films had an electron concentration of $1.1 \times 10^{18} \text{ cm}^{-3}$.

Chapter 4

Device Structure and Fabrication

4.1 Tandem Cell Structure

A tandem solar cell usually has two cells having different band gaps placed one over other with an encapsulant between them. They are designed in such a way that the top cell has a larger band gap and hence can absorb lower wavelengths. The bottom cell with a relatively smaller band gap can absorb higher wavelengths that pass through the top cell. A 4 - terminal tandem solar cell structure is shown below

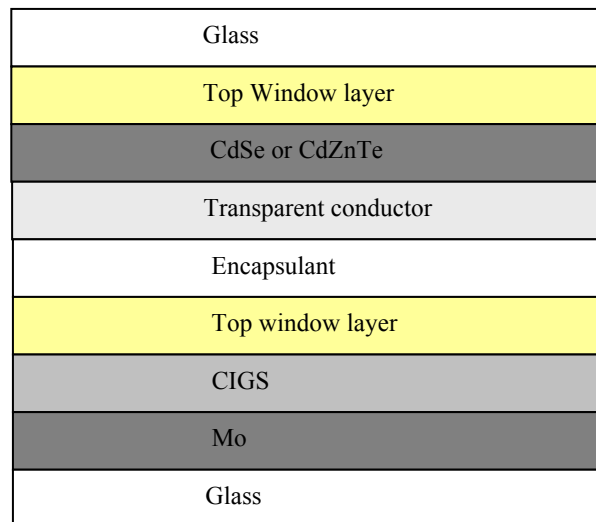


Fig 4.1 Tandem Solar Cell Structure

To obtain efficiencies greater than 25 %, the top cell should have a bandgap of 1.7 eV. This would mean that the top cell has to contribute to 2/3 rd of total efficiency. The bottom cell of the tandem structure having a bandgap of 1 eV has already been standardized. CIGS solar cells with a bandgap of 1 eV have attained an efficiency of 18 %.

Though there are a few of I-III-VI₂ compounds like CuGaSe₂ with a band gap of 1.7 eV and CuInS₂ with a bandgap of 1.55 eV, they cannot be used for the top cell because of their relatively lower efficiencies [21, 30]. Other materials being investigated as viable candidates for the top cell are Cd_{1-x}Zn_xTe and CdSe. Cd_{1-x}Zn_xTe is a ternary alloy with a tunable bandgap. CdSe is also found to be another suitable material to serve as the absorber layer in the top cell [3]. P.Gashin et al fabricated a 3 - terminal monolithic tandem structure of n-ZnSe/p-ZnTe/n-CdSe and reported an efficiency of 10.8 % [22].CdSe can be processed with lesser complexity when compared to any I-III-VI₂ compound. This thesis focuses on the development of a top cell with CdSe as an absorber layer. The top cell of the proposed tandem solar cell should have a superstrate structure. But for initial experiments we started of with a substrate structure.

4.2 Structure of a CdSe Based Top Cell

The structure of a CdSe based top cell is shown below.

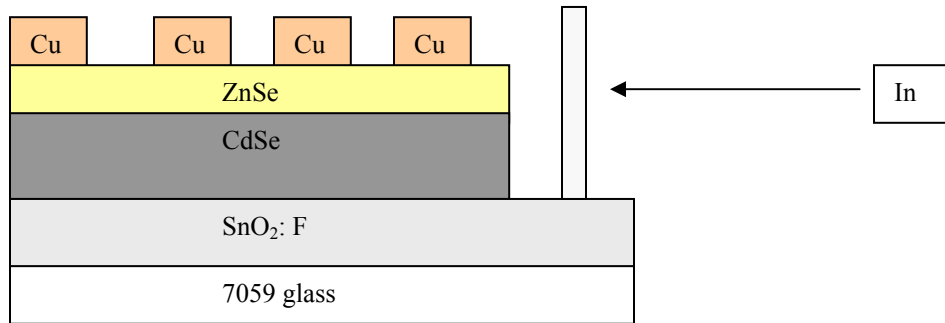


Fig 4.2 Structure of CdSe Based Top Cell

4.2.1 Substrate

In our process we use Corning 7059 glass substrates because of their stability to withstand high temperature processing above 700°C. Typical dimensions of the substrate are 1.25 X 1.35 X 0.05 inches.

4.2.1.1 Cleaning Procedure

Before any deposition process, the substrate goes through a regular cleaning procedure. This is a very important step in processing. Any contaminants present on the substrate could affect the subsequent deposition steps and the device performance. The substrate is first dipped in dilute HF (1 part of HF in 10 parts of water) for 5 seconds, rinsed under a jet of DI water. It is again dipped in dilute HF for 3 seconds and is finally rinsed under a jet of DI water. It is then blown dry with nitrogen.

4.2.2 Back Contact

A good back contact should be transparent, conductive and have the proper contact energy. SnO₂: F and AZO are the two TCO's used as back contacts.

SnO₂: F has a band gap of 3.5 eV. It is a very good TCO because of its high transmission of 90 % and low sheet resistance of 7-10 ohms/sq. The transmission response of SnO₂: F is shown in Fig 4.3.

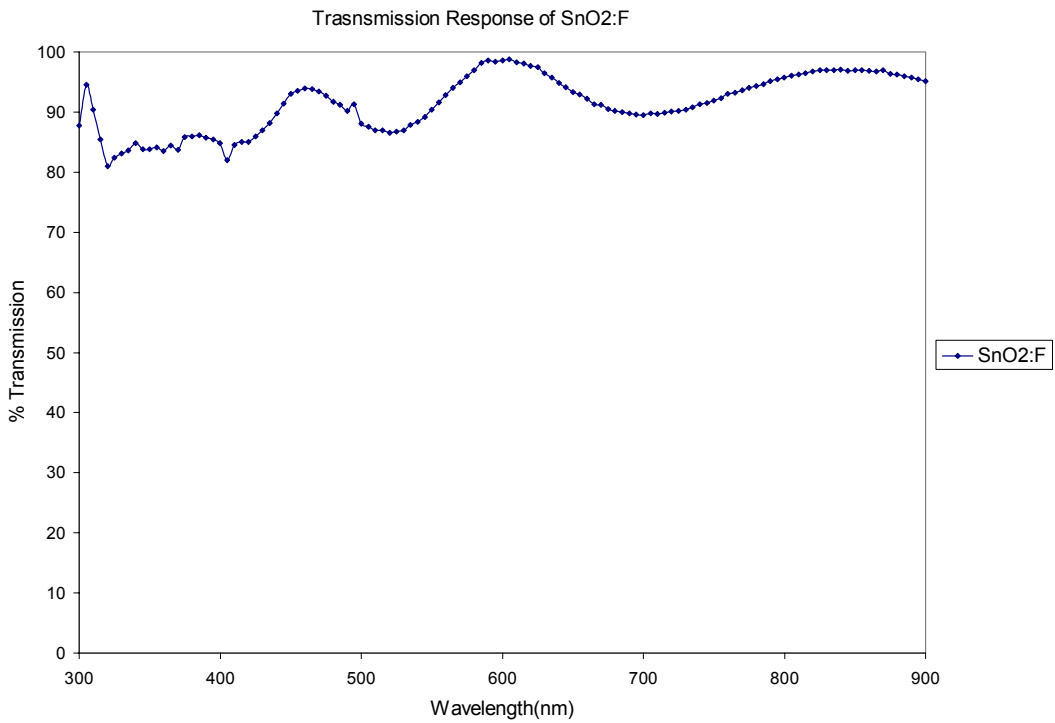


Fig 4.3 Transmission Response of SnO₂: F

4.2.2.1 Deposition of SnO₂: F

SnO₂: F is deposited by MOCVD. TMT (Tetra Methyl Tin) is used as the source for Tin. Halocarbon 13B1 is used as the source for Fluorine which acts as the dopant. The substrate is heated to 470° C. For the first 8 minutes-TMT, Halocarbon 13B1 and oxygen are reacted to deposit a doped layer of SnO₂. This layer is n-type. For the next 5 minutes, the substrates are annealed in the presence of oxygen. For the last 5 minutes an undoped layer of SnO₂ is deposited. In order to overcome problems due to diffusion an undoped layer of SnO₂ is deposited. The thickness of the film is approximately 800 Å.

4.2.2.2 AZO as a Back Contact

AZO with a bandgap of 3.3 eV has also been used as a back contact. The following properties of AZO make it a viable back contact.

- 1) Raw materials required are cheap and abundant.
- 2) They have a very high transmittance reaching close to 90 % in the visible region.
- 3) They are readily produced for large scale coatings.
- 4) They have high stability in hydrogen plasma.
- 5) They have low growth temperature.
- 6) They have a very low resistivities of order $1.4 \times 10^{-4} \Omega\text{-cm}$.

The conductivity of ZnO is primarily dominated by electrons generated from oxygen vacancies and Zn interstitial atoms. The electrical conductivity in AZO films is more than

ZnO films due to the added contribution from Al^{+3} ions on substitutional sites. ZnO films have polycrystalline hexagonal wurtzite structure as shown in Fig 4.4.

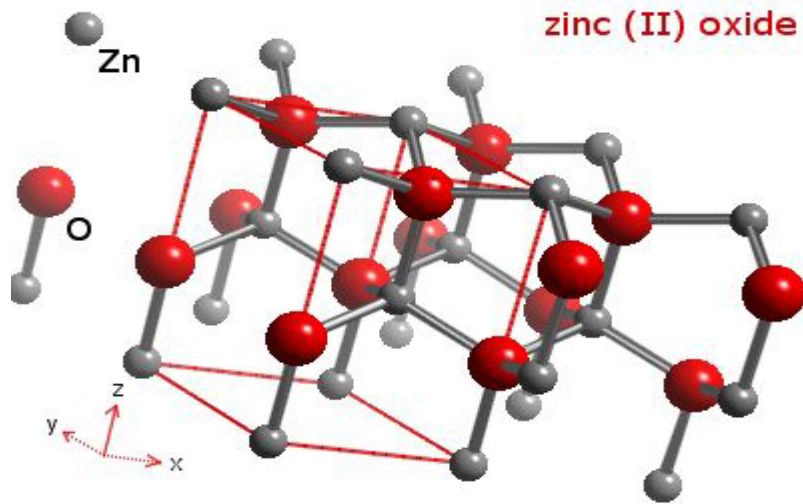


Fig 4.4 Wurtzite Structure of Zinc Oxide

4.2.2.3 Structure of Cell with AZO at the Back Contact

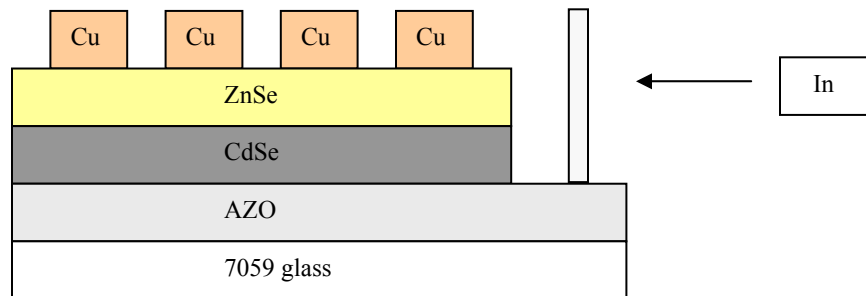


Fig 4.5 Structure of Cell with AZO at the Back Contact

Aluminum doped Zinc oxide is deposited on Corning 7059 glass substrates. CdSe is deposited on AZO by close space sublimation in the chamber shown in Fig 4.11. ZnSe and Copper are deposited by Thermal Evaporation in the chamber shown in Fig 4.14.

4.2.2.4 Deposition Procedure for AZO

AZO films are deposited by R.F Magnetron Sputtering. A cleaned 7059 glass substrate is loaded in the chamber. The chamber is pumped to low micro Torr range. The substrate is heated to 125° C through a specific heating profile by a variac. A ZnO (2 % wt Al₂O₃) target is sputtered in the presence of argon. To begin with, 2000 Å thick films were deposited. Later on the thickness of the films was increased to 5000 Å. Transmission of about 90 % with a resistivity of $4 \times 10^{-4} \Omega\text{-cm}$ has been achieved.

4.2.2.5 Transmission of AZO

The transmission response of AZO films having a thickness of approximately 5000 Å is shown in Fig 4.6. We can observe that in the wavelength region between 450 and 900 nm there is a high transmission of about 90 %. Because of its good optical properties, AZO is a good choice for the TCO layer.

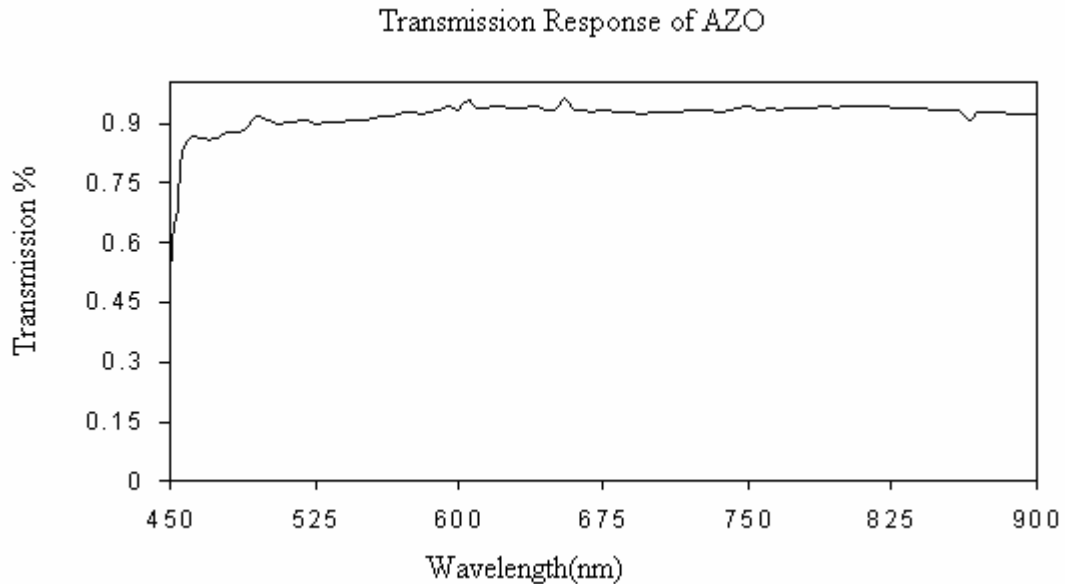
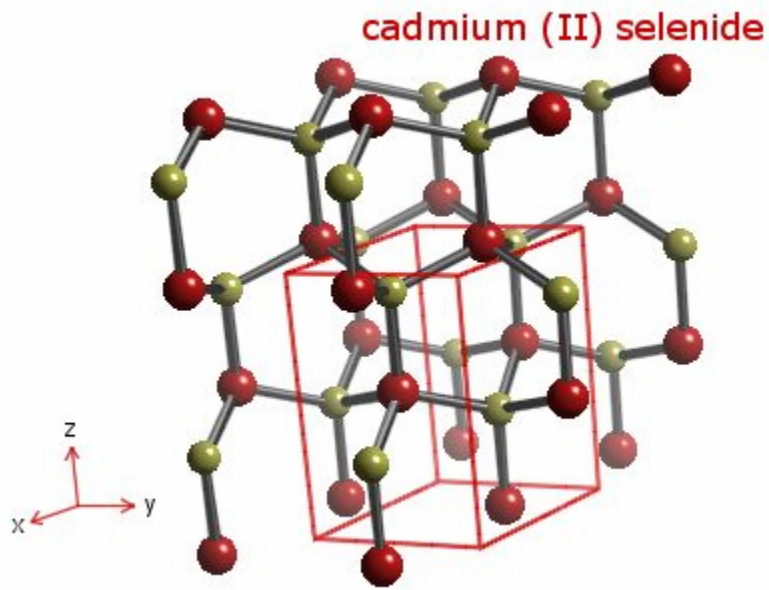


Fig 4.6 Transmission Response of AZO

4.2.3 Absorber Layer

Due to its high electronic quality and a fixed optical bandgap of 1.7 eV, Cadmium Selenide is chosen as one of the materials that can be used as an absorber layer in the top cell. It belongs to II-VI group of the periodic table. Cd has 2 electrons in its outer most orbit while Se has 6 electrons. Every Cd atom transfers its 2 electrons to 6 valence electrons of Se to form CdSe. A vacancy of a Selenium atom frees two electrons of Cadmium making CdSe n-type.



4.7 Wurtzite structure of CdSe

CdSe crystallizes either in wurtzite (Hexagonal) or cubic (Zinc blende) structures. The wurtzite structure of CdSe is shown in the Fig 4.7. CdSe deposited as a part of this work has Hexagonal structure which was demonstrated from the AFM image shown in Fig 4.8.

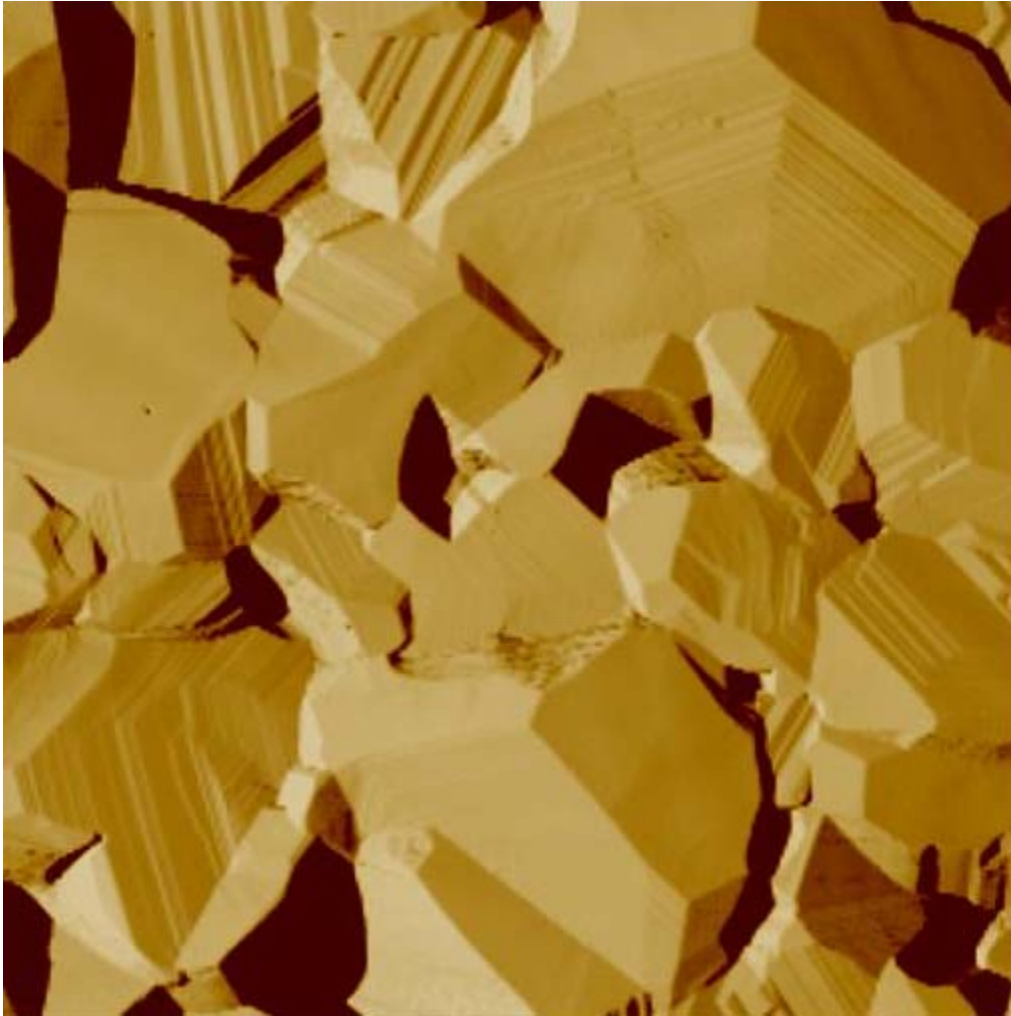


Fig 4.8 AFM image of CdSe

From the AFM image we can notice the hexagonal planar structure of the CdSe film. The dark regions in the image are grain boundaries. Usually, the larger the grain size the better the quality of the films. Larger grain sizes also result in the improvement of the transport properties of minority charge carriers.

4.2.3.1 Properties of CdSe

Table 4.1 Properties of CdSe

Bandgap	1.74 eV
Electron Affinity	4.56 eV
Lattice constant	6.05 Å

4.2.3.2 Preparation of the CdSe Source

High purity (99.999%) CdSe powder is used in the preparation of the source. Enough care is taken so that there are no contaminants present that could affect the device performance. A circular disk of 2 mm thick and 1 inch in diameter is prepared by pressing CdSe powder in a circular mold.

4.2.3.3 Deposition Procedure for CdSe

CdSe can be deposited by various methods like Thermal evaporation, Chemical vapor deposition, Sputtering, CBD, Electrodeposition and CSS. CSS is not only a simpler process but can also produce films of good electronic properties. The deposition rate is high so that 1-2 μ m thick films can be deposited in a short time. The source is kept on a graphite holder and is separated from the substrate by quartz spacers. Each of the two quartz lamps is fixed to a reflector. Lamps are placed one over the other so that most of the heat is localized. The setup is shown in Fig 4.9.

The reactor tube is pumped to less than 1 Torr by a mechanical pump and is purged with Helium for couple of times. Finally it is back filled with Helium to a

pressure of 3 Torr. The source and the substrate temperatures are set using a temperature controller. Both the lamps are turned ON. When source and substrate temperatures reach their set values, sublimation begins and the time for the sublimation is noted. Both the lamps are turned OFF as soon as the deposition time is over.

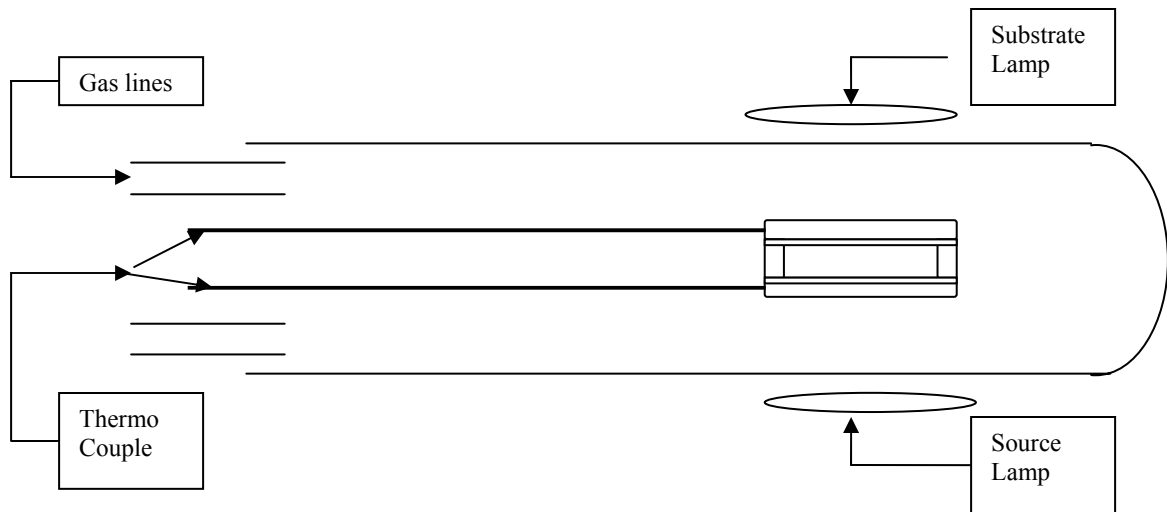


Fig 4.9 Closed Space Sublimation Setup

4.2.3.4 Parameters

CdSe was deposited under different conditions. The quality of the films was optimized by varying parameters like pressure, source temperature, substrate temperatures and spacing. The optimized parameters are:

$T_{\text{sou}}-670^{\circ}\text{C}$

$T_{\text{sub}}-560^{\circ}\text{C}$

Ambience used-He

Pressure-3 Torr

$t_{\text{deposition}}$ - 14 minutes.

The thickness of the film obtained for the above conditions is around 1.5 microns.

4.2.3.5 Transmission of CdSe

The transmission response of CdSe films deposited under standard conditions is shown in Fig 4.10. From the transmission response measurements; we can notice that the films have approximately 80 % transmittance between 750 and 900 nm. CdSe absorbs high energy photons and transmits the low energy photons to the bottom cell. The cutoff wavelength is at 725 nm which corresponds to the band gap of CdSe.

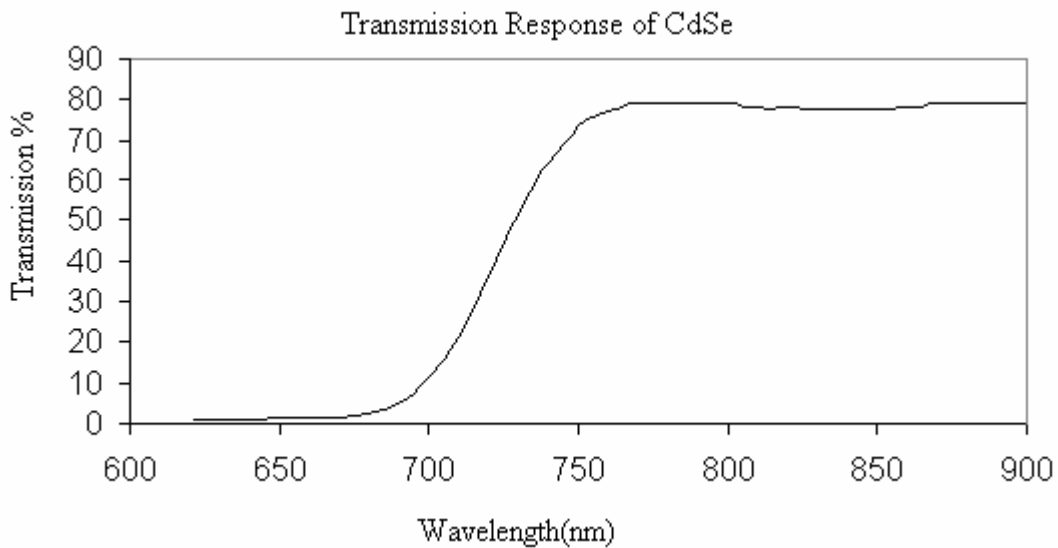


Fig 4.10 Transmission Response of CdSe

4.2.3.6 Experiments Performed on the Absorber Layer

The source is sublimated at different temperatures from 630° C to 670° C. The films obtained at 630° C were not uniform but as the source temperature is increased to 670° C, uniformity of the films improved. This could be because at high temperature

the source gets the required energy to disassociate into fine particles and then sublimate into a uniform layer of CdSe.

Similarly the substrate temperature was maintained at 560° C for standard runs. Under standard conditions the film thickness was about 1.5 μm . Further experiments were performed by elevating the substrate temperature in steps of 10° C starting from 560° C.

Substrates at higher temperatures have higher energies associated with them, and therefore atoms from the source do not tend to stick. Hence the thickness of the film decreased with the increase in the substrate temperature. Sticking of the material depends on the type of material that is being deposited and the type of substrate on which the film is growing. The coefficient of sticking varies from material to material.

4.2.4 Window Layer

In order to transmit the maximum amount of light to the absorber layer, we need a window layer with a high bandgap. Zinc Selenide with a band gap of 2.7 eV can be used as a window layer. It is a II-VI semiconductor widely used in many opto-electronic applications. The crystal structure of ZnSe is shown in Fig 4.11. It crystallizes into a Zincblende structure.

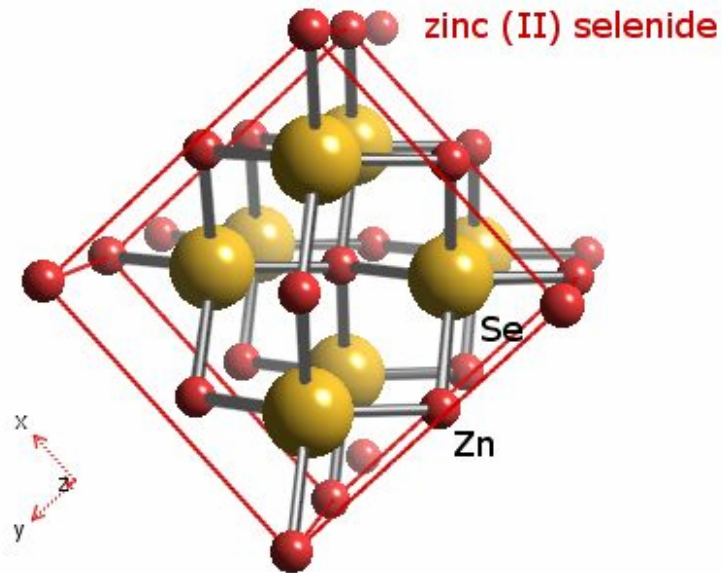


Fig 4.11 Structure of ZnSe

4.2.4.1 Properties of ZnSe

Table 4.2 Properties of ZnSe

Bandgap	2.7 eV
Electron Affinity	4.1 eV
Lattice constant	5.668 Å

4.2.4.2 Deposition Procedure for ZnSe

High purity (99.999%) ZnSe powder is used as the source which is thermally evaporated. A specific voltage-time profile is followed for heating the source. ZnSe films are deposited at two different substrate temperatures- at room temperature and at 250° C. The devices fabricated with ZnSe deposited at 250° C did not show good performance whereas the devices fabricated with ZnSe at room temperature have shown good performance. All the films in this work are grown at room temperature.

4.2.4.3 Evaporation System

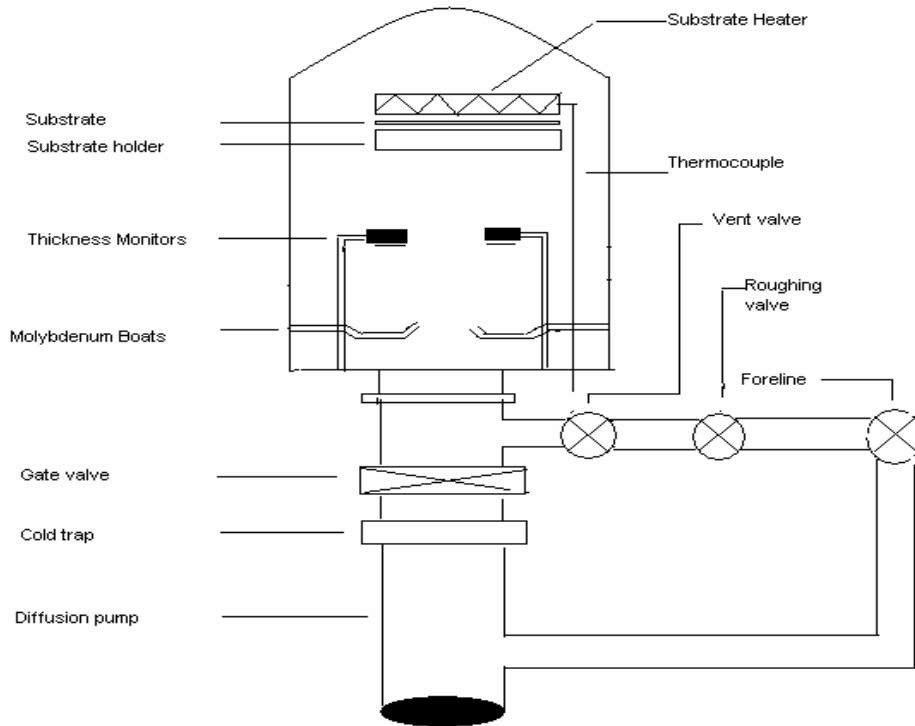


Fig 4.12 Evaporation System

The Evaporation system shown in Fig 4.12 is equipped with a diffusion pump and a Mechanical pump to evacuate the chamber to the micro Torr range. A cold trap separates the chamber and the diffusion pump. Liquid Nitrogen is filled in regular intervals to trap moisture.

There are two Molybdenum boats-one for ZnSe and the other for Copper. These boats are resistively heated.

4.2.4.4 Transmission of ZnSe

The transmission response of ZnSe is shown in Fig 4.13. The thickness of the film is 200 Å. There is a significant absorption in the blue region of the spectrum which can be clearly observed. We can notice from Fig 4.13 that ZnSe has approximately 90 % transmission in the visible region which makes it a good choice for the window layer.

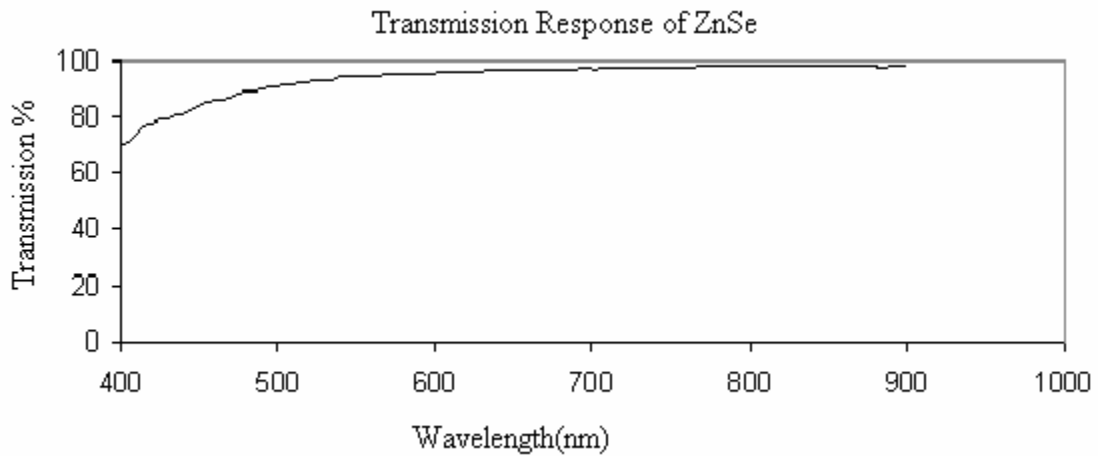


Fig 4.13 Transmission Response of ZnSe

4.2.5 Front Contact

The material used as the front contact must be conductive, transparent and make an ohmic contact with ZnSe. Copper is deposited as front contact by Thermal Evaporation in the chamber shown in Fig 4.13. Copper pellets (99.999% pure) are added to the front boat in the chamber. A mask of 0.1 cm² area dots is used for depositing copper on the ZnSe film. The chamber is initially pumped to the micro Torr range. The source is heated using a variac following a specific voltage-time profile.

4.2.5.1 Transmission of Copper

The transmission response of copper is shown in Fig 4.14. The thickness of the film is 60 Å. Since Copper is a metal, most of the light incident on the surface will be reflected if the film is too thick. So at lower wavelengths most of the incident light is reflected, and hence the transmittance is less.

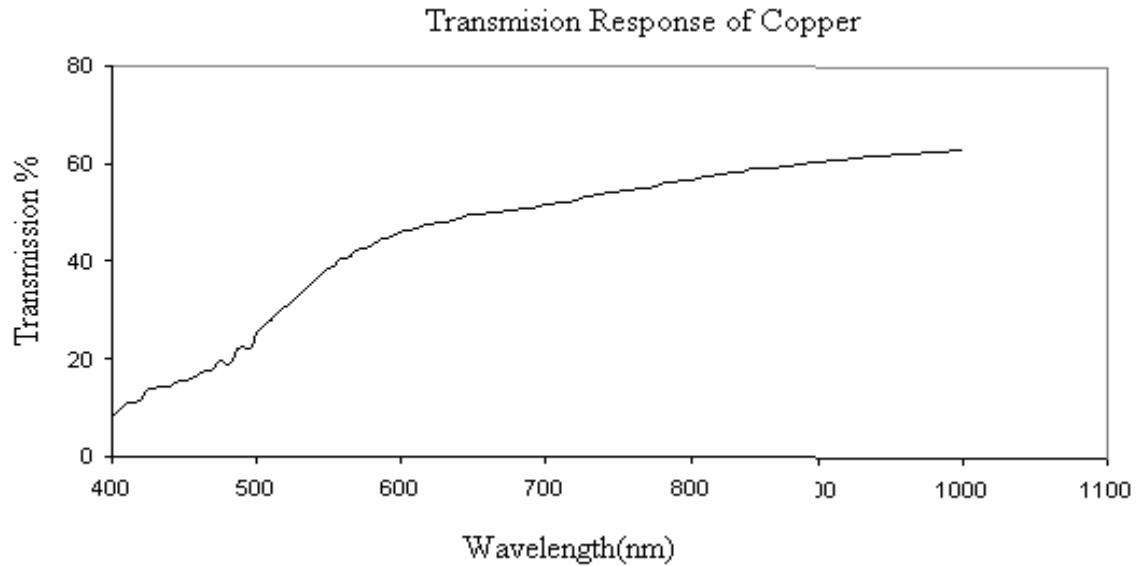


Fig 4.14 Transmission Response of Copper

4.3 Deposition of Cadmium Sulphide

CdS is a direct band gap material. CdS films have a wurtzite structure as shown in Fig 4.15 and has a band gap of 2.4 eV.

CdS can be deposited by different methods like close space sublimation, chemical bath deposition and sputtering. CBD is popular among the three since it gives uniform films. The process is simple and inexpensive compared to an expensive vacuum deposition.

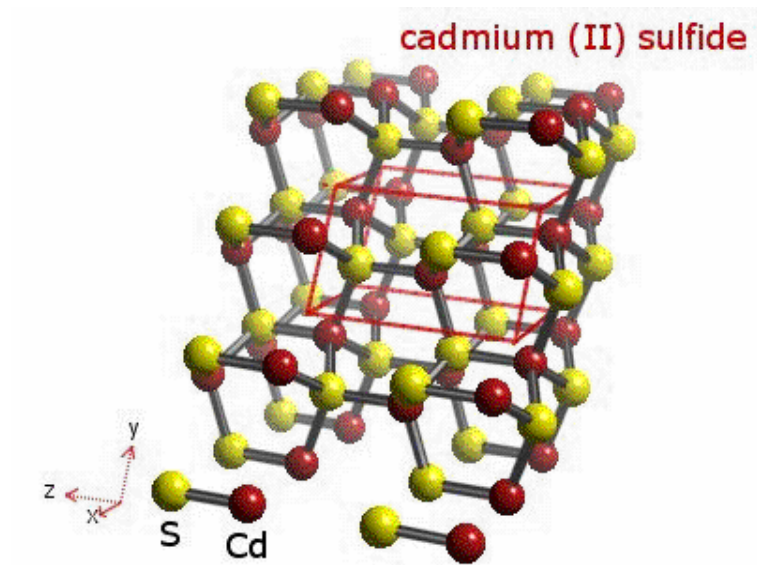


Fig 4.15 Structure of CdS

For the results presented below, CdS is deposited by CBD. Thiourea, Ammonium Hydroxide and Cadmium acetate are chemicals used in the reaction. Cadmium acetate is used as a source for cadmium. Thiourea is used as a source for Sulphur. The growth rate of CdS depends on deposition temperature and the pH of the solution.

The precipitation temperature is around 87° C. For a deposition time of 80 minutes, a thickness of around 1000-1200 Å is deposited on the substrate. CdS of thickness around 300- 500 Å is deposited on SnO₂: F to fabricate the same structure as shown in Fig 4.17.

4.3.1 Transmission of CdS

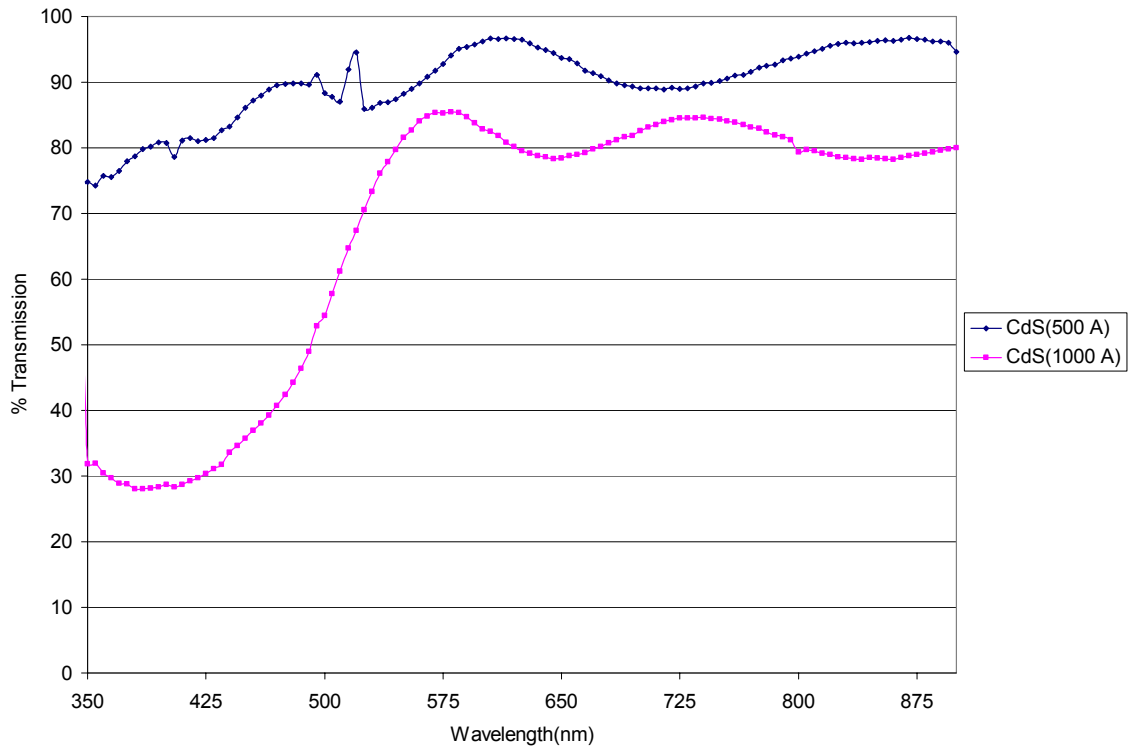


Fig 4.16 Transmission Response of CdS

CdS of thickness around 500 Å and 1000 Å is deposited by CBD on SnO₂: F substrates. SnO₂: F is used as reference for the transmission measurements. From Fig 4.16, we can notice that the transmission of thin CdS is above 90 % whereas the thick ones have a transmission of 85 %. This loss is due to the absorption in CdS.

4.3.2 Structure of Cell with CdSe on CdS/SnO₂: F

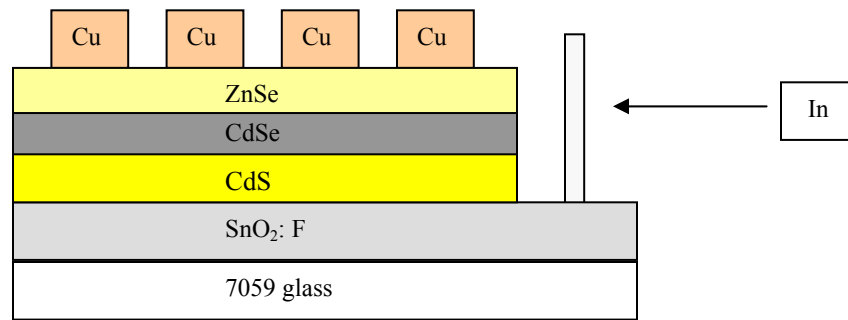


Fig 4.17 Structure of Cell with CdSe on CdS/SnO₂: F

A uniform film of CdS is deposited by CBD. When SnO₂: F substrates are placed in the chemical bath during CBD, CdS is deposited on both sides of the substrate. CdS on the other side of SnO₂: F is chemically etched by a cotton swab dipped in dilute HCl. A narrow strip of CdS is etched on the SnO₂: F in order to put an Indium contact.

Chapter 5

Results and Discussions

5.1 Results

Devices fabricated are measured to study their responses in light and dark illumination conditions.

5.1.1 AZO as a Back Contact

Devices with AZO as a back contact are fabricated and annealed at 100° C for 10 minutes. The performance of the devices before and after annealing is shown in Table 5.1. The J-V response for the device sh18-g before and after annealing is shown in Fig 5.1(a) and 5.1(b) respectively. The effect of annealing on the J-V response of the devices can be clearly seen.

Table 5.1 Device Parameters for Devices with AZO as a Back Contact

Before Annealing			After Annealing		
Sample #	Voc(V)	FF	Voc(V)	FF	J _{sc} (mA/cm ²)
sh18-g	0.210	30	0.370	50.2	5.19

From the J-V curve we can notice that the Voc and FF have increased after annealing the sample. From the dark J-V curve we can notice that the devices turn on

slowly after annealing. The devices had lower shunt resistance before annealing. After annealing the shunt resistance has improved but the series resistance remained almost the same. The low shunt resistance before annealing could be due to high leakage currents.

Annealing could have improved the interface between CdSe/ZnSe which resulted in increased Voc and FF. It was observed that annealing of AZO films at high temperatures has resulted in increased resistivity. As the deposition of CdSe involves high temperature processing, this could have deteriorated the properties of AZO films resulting in high series resistance of the devices.

Sh18(7059/AZO-5000 Å /CdSe-670 C,560 C,3 T He-14 min/ZnSe-380 Å/Cu-40 Å)

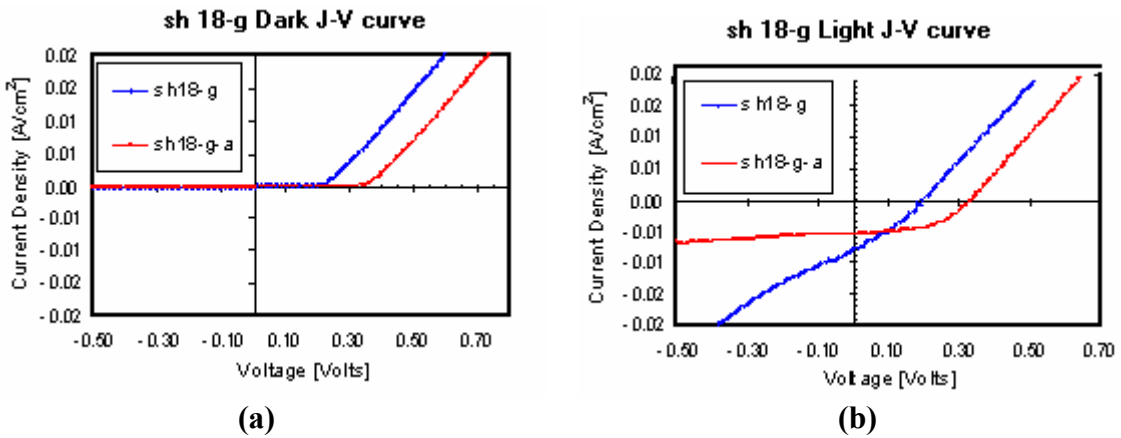


Fig 5.1(a) and (b) J-V Curve for Device # sh18-g

The spectral response of sh18-g is shown below in Fig 5.2.

sh 18-g (7059/AZO-5000 Å/CdSe-670 C,560 C,3 T He-14 min/ZnSe-380 Å/Cu-40 Å

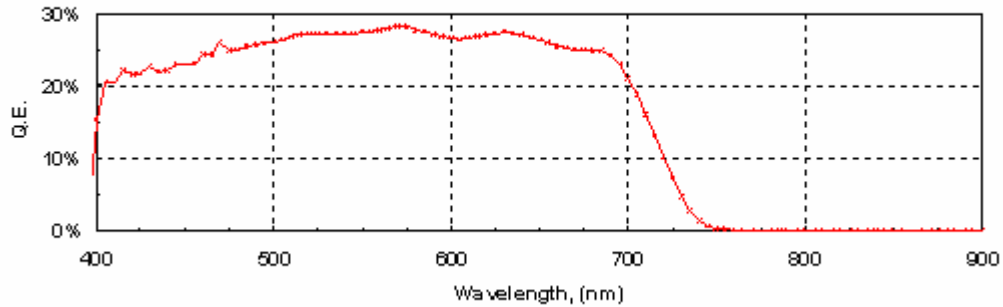


Fig 5.2 Spectral Response for Device # sh18-g

From Fig 5.2 we can observe that the Q.E is less than 30 %.Though in the wavelength region between 500 nm and 700 nm Q.E is flat, there is a considerable absorption in the blue region. This is because of the absorption by ZnSe. The response cutoff at 725 nm corresponds to the fundamental band gap of CdSe. As the Q.E's are approximately around 30 %, J_{sc} 's are relatively low.

5.1.2 CdS on SnO₂: F at the Back Contact

CdS is deposited on SnO₂: F. n+ CdS makes the other side of the junction more n type. This increases the band bending which results in improved open-circuit voltages. Table 5.2 shows the results of the cells with CdS of thickness 500 Å and 1000 Å deposited on SnO₂:F.Devices were annealed in air at 100° C for 10 minutes.

Devices with thinner CdS show poor performance before annealing. This can be because thinner CdS may not have uniformly covered the rough surface of the back contact. After annealing Voc and FF have improved. This could be because surface

properties might have improved resulting in a better interface between SnO₂: F/CdS. Annealing could also have improved the junction between CdSe/ZnSe by reducing the interface traps.

Table 5.2 Device Parameters for Devices with CdS on SnO₂: F at Back Contact

Before Annealing				After Annealing		
Sample	Thickness of CdS in Å)	Voc(V)	FF	Voc(V)	FF	Jsc(mA/cm2)
Sh39-1-a	500	0.270	18	0.320	50.2	7.52
Sh40-1-e	1000	0.330	55.1	0.350	47.5	7.21

J-V response for the device fabricated with 500 Å thick CdS is shown in Fig 5.3(a) and Fig 5.3(b).

Sh39-1-a(7059/SnO₂: F- 800 Å /CdS-500 Å /CdSe-670°C,560°C,3T He-14min/ZnSe-200 Å /Cu-30 Å)

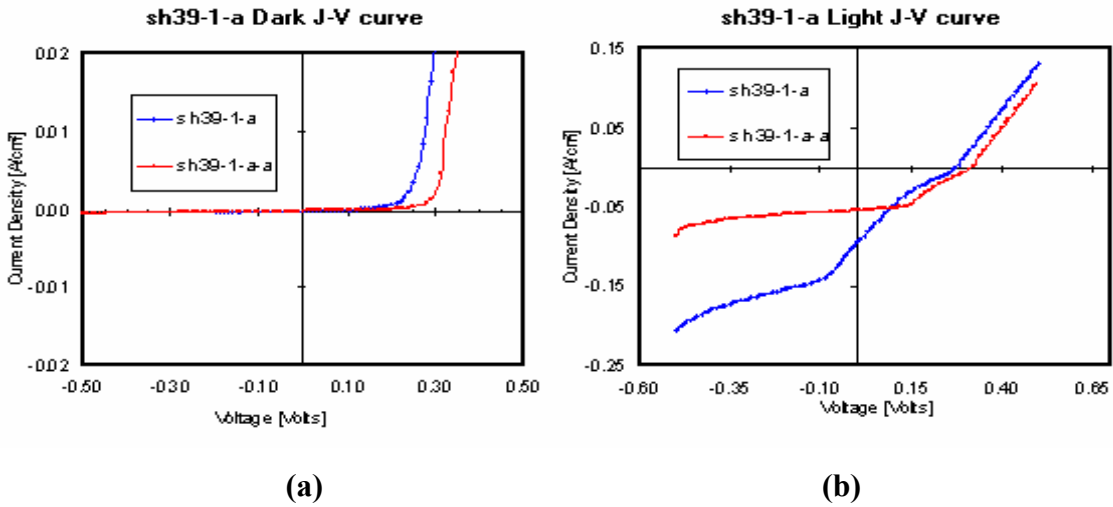


Fig 5.3(a) and (b) J-V Curve for Device # sh39-1-a

Devices with thicker CdS have shown better performance even before annealing. Thicker CdS may have uniformly covered the rough back contact. This makes the other

layers grow more uniformly increasing the junction and surface properties. Annealing has not shown a considerable improvement in the performance. The increase in Voc after annealing could be due to the passivation of interface traps. This could have reduced the leakage currents.

J-V response for the device with 1000 Å CdS is shown in Fig 5.4(a) and Fig 5.4(b).

Sh40-1-e(7059/SnO2-800 Å /CdS-1000 Å /CdSe-670 C,560 C,3 T He-14 min/ZnSe-200 Å /Cu-30 Å)

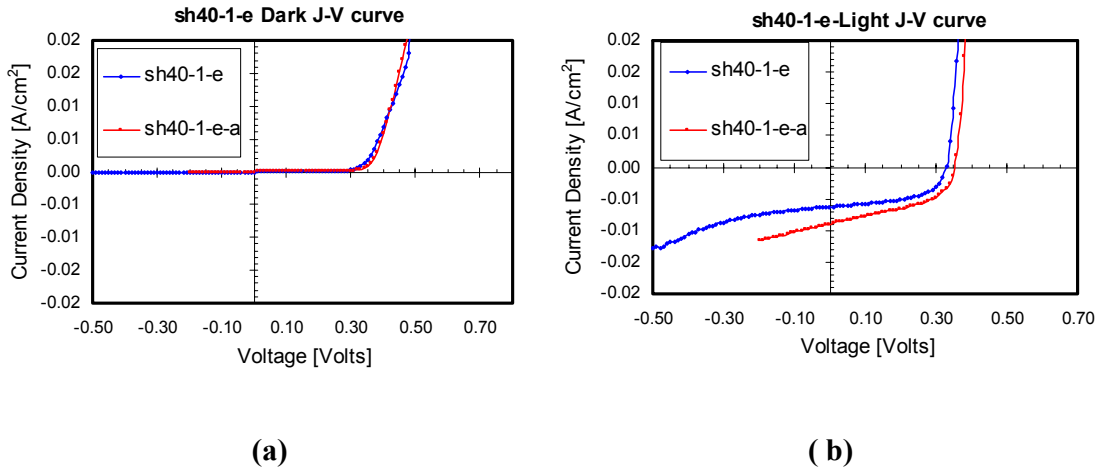


Fig 5.4 (a) and (b) J-V Curve for Device # sh40-1-e

From the J-V curve we can also confirm that the Fill factors are comparable before and after annealing. Spectral response of both the devices is shown in Fig 5.5.

sh39-1-a (7059/SnO₂:F-800 Å/CdS-500 Å/CdSe-670C,560C,3T He-14min/ZnSe-200 Å/Cu-30Å)
sh40-1-e(7059/SnO₂:F-800 Å/CdS-1000 Å/CdSe-670C,560C,3T He-14min/ZnSe-200 Å/Cu-30Å)

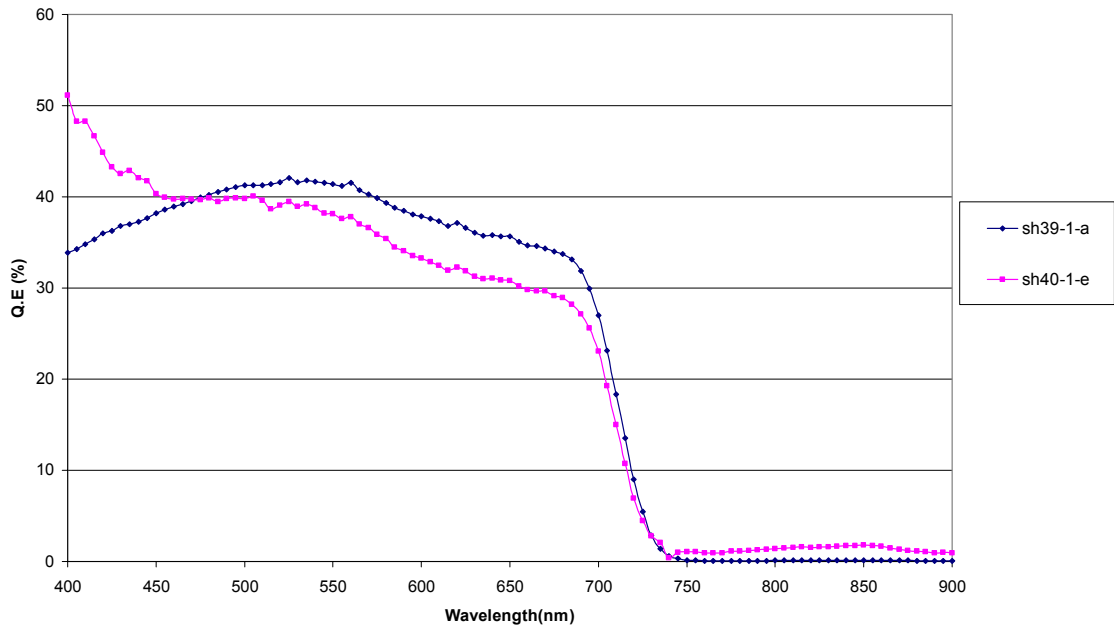


Fig 5.5 Spectral Response for Device # sh39-1-a and # sh40-1-e-a

For the device with CdS thickness around 500 Å in the shorter wavelengths Q.E is around 35 %.The device with CdS thickness around 1000 Å has collection problems and hence has lower Q.E in higher wavelengths.

5.1.3 Absorber Layer at Higher Substrate Temperatures

During the J-V measurements when the light is incident through SnO₂: F none of the cells showed any response. So to allow more light to pass through the back contact and reach the absorber layer, the thickness of the absorber layer has been decreased. To make films thin, the substrate temperature was raised from 560°C. This section shows the experiments performed on the absorber layer by sublimating at higher substrate

temperatures. But the devices when measured for light J-V did not show any response when light is incident through SnO₂:F. So their response to J-V measurements when light is incident through Copper is studied. V_{oc}'s and J_{sc}'s are given in Table 5.3

Thickness of the ZnSe film is 200 Å.

Table 5.3 Effect of Substrate Temperature on Device Performance with 200 Å ZnSe

Sample	Tsub(C)	Voc(V)	FF	Jsc(mA/cm2)
sh52-1-f	560	0.130	35.2	9.48
sh48-2-l	570	0.150	16.5	6.27
sh44-1-f	580	0.270	33.3	5.42
sh45-1-e	590	0.160	48.6	8.58

Light J-V curves for the above substrates are shown in Fig 5.6.

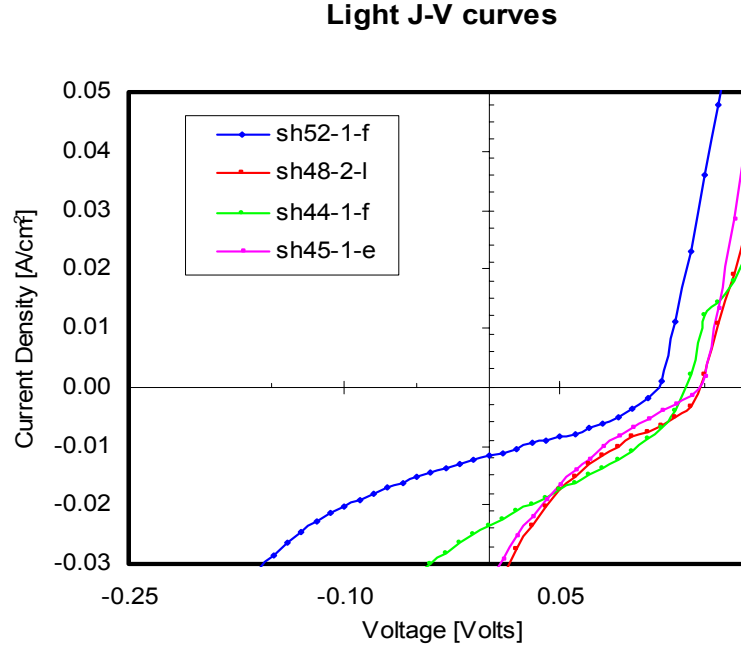


Fig 5.6 J-V Curve for the Devices # sh44-1-f, # sh45-1-e, # sh48-2-l and sh52-1-l

From the J-V plots, it can be seen that these devices had higher series and low shunt resistances. As the substrate temperature is increased from 560° C to 590° C, V_{OC} 's have improved with the highest V_{OC} around 270 mV for a substrate temperature of 580° C in sample sh44-1-f. On the other hand, J_{SC} is highest for sample sh52-1-f of 9.48 mA/cm². At 590° C, the current density is reasonable. At 590° C V_{OC} 's tend to fall. All the above devices have low fill factors because of their series and shunt resistances. But the above devices did not follow any particular trend in their performance.

As a part of further experimentation, the thickness of ZnSe is increased to 220 Å to observe its effect on device performance.

Thickness of ZnSe film is 220 Å.

Table 5.4 Effect of Substrate Temperature on Device Performance with 220 Å ZnSe

Sample	Tsub(°C)	Voc (V)	FF	Jsc (mA/cm ²)
sh49-2-f	580	0.190	50.0	8.4
sh50-2-e	590	0.230	72.4	9.11
sh53-1-l	610	0.110	37.9	7.48

The high fill factor in sh49-2-f and sh50-2-e is due to the sharp turn in light J-V shown in Fig 5.7. In a MIS type structure, ZnSe acts as an insulating layer. When copper is deposited on ZnSe there is a chance of diffusing into the insulating layer which might lead to formation of homogenous p-type material [30]. This could result in higher built-in potential hence improving the open-circuit voltages. But if the amount of copper

deposited is not sufficient to make a p-type contact to the absorber layer, or if the thickness of ZnSe is not in proportion with the thickness of copper then there cannot be any significant improvement in Voc's.

As the substrate temperature is increased, the structural properties of the films may change. Generally it is expected that the films obtained at higher substrate temperatures are more crystalline in nature and hence have better properties [16]. But on the other hand if the temperature is increased further, films may become amorphous affecting the photovoltaic properties of the devices.

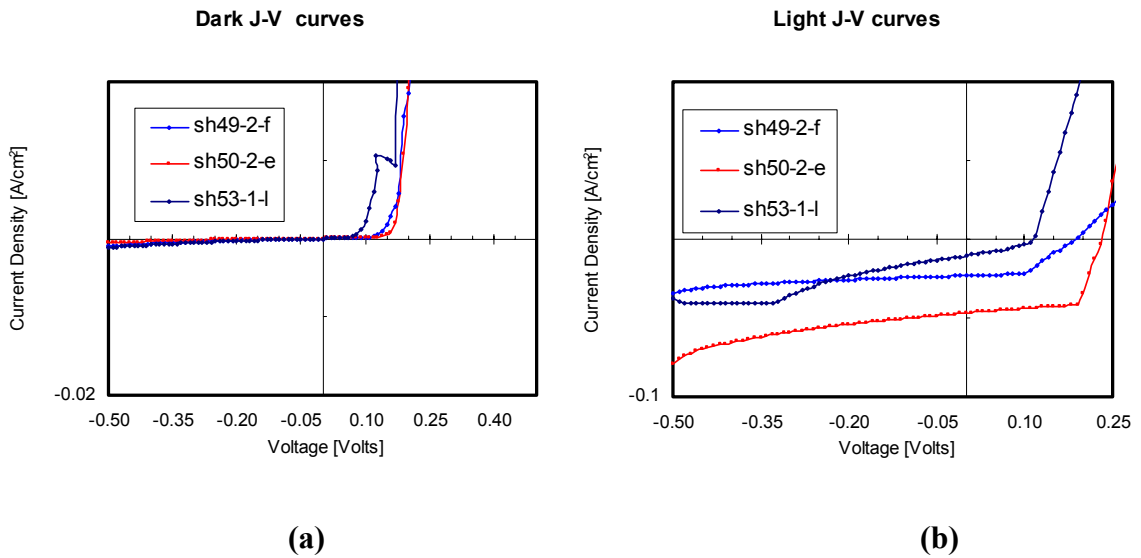


Fig 5.7 (a) and (b) J-V Curve for Devices # sh49-2-f, # sh50-2-e and # sh53-1-l

Table 5.5 Effect of Substrate Temperature on Device Performance with 180 Å ZnSe

Sample #	T _{sub} (°C)	Voc (in V)	FF	J _{sc} (mA/cm ²)
sh49-3-b	560	0.220	33.8	10.02
sh51-2-c	600	0.220	71.8	5.76

Both these devices had Voc's of around 220 mV. From the light J-V of sh49-3-b in Fig 5.8, it can be observed that the series resistances are high and shunt resistances are low. This device has obtained a highest J_{sc} of 10.02 mA/cm². If the shunt resistance values can be increased, J_{sc}'s may be improved further. sh51-2-c has low J_{sc} but Voc's are comparable. The spectral response of devices sh50-2-e, sh49-3-b and sh52-1-f are shown in Fig 5.9

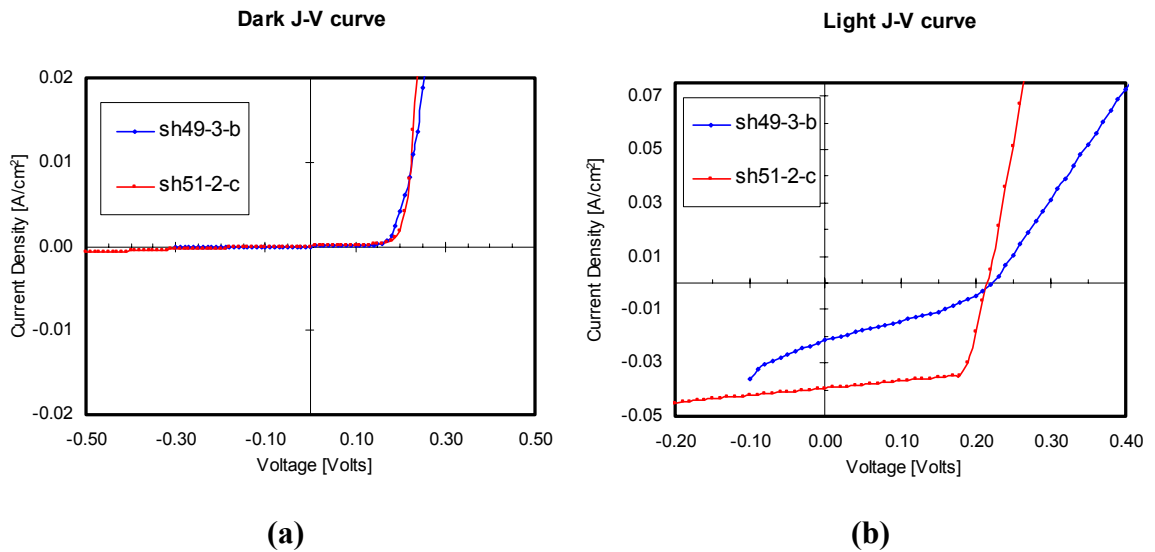


Fig 5.8 (a) and (b) J-V Curve for the Devices # sh49-3-b and # sh51-2-c

sh50-2-e(7059/SnO₂:F-800 A/CdSe-670 C,590 C,3 T He-14 min/ZnSe-220 A/Cu-30 A)
sh49-3-b (7059/ SnO₂:F -800 A/CdSe-670 C,560 C,3 T He-14 min/ZnSe-180 A/Cu-30A)
sh52-1-f (7059/ SnO₂:F -800 A/CdSe-670 C,560 C,3 T He-14 min/ZnSe-200 A/Cu-30 A)

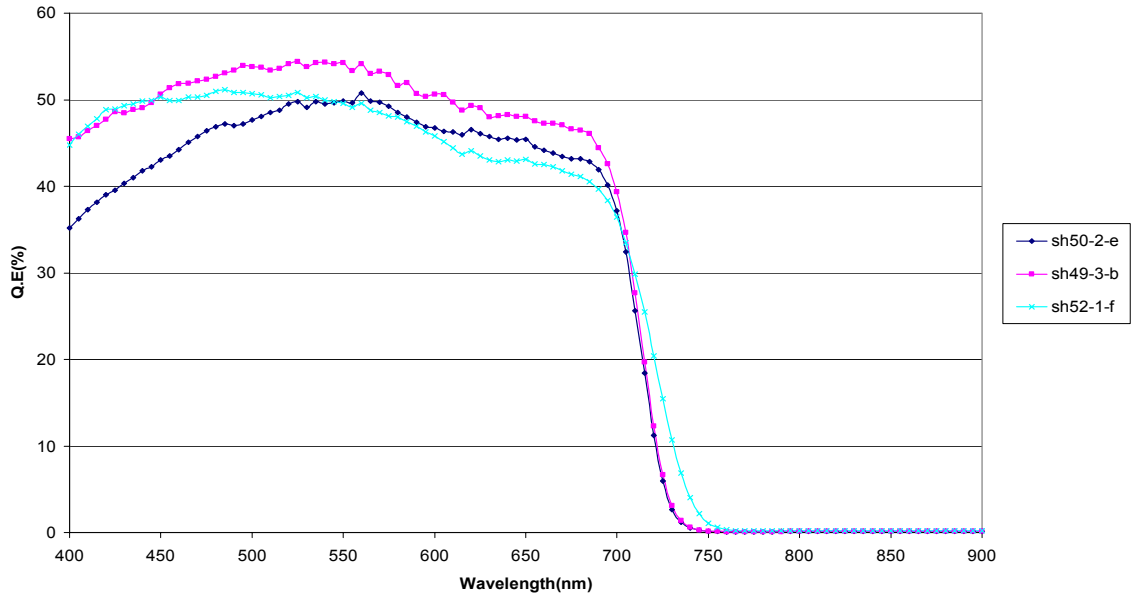


Fig 5.9 Spectral Response for Devices # sh50-2-e, #sh49-3-b and # sh52-1-f

The Q.E of sh50-2-e is lower in comparison with the other two devices. This is because of the absorption in the blue region. This device has higher absorption in the blue region due to thicker ZnSe. It is observed that the thickness of copper and ZnSe is crucial for the performance of these devices. If the thickness of copper is more than the standard thickness, then there is a chance of copper diffusing through the junction and shorting the devices. If the thickness of copper is less, it was observed that the open circuit voltages obtained was less. If the optimum thickness of copper is deposited on ZnSe, it can enhance the photo-voltaic properties of the devices. Hence optimization of the thickness of copper is important .We have varied the thickness of copper from 60 Å to 30 Å.

The highest Q.E of around 55 % is obtained for sh49-3-b at mid wavelengths. The carrier collection in the mid wavelengths is good resulting in higher Jsc's compared to the remaining devices.

5.1.4 Effect of Time on Device Performance

It was observed that the devices fabricated have shown better photovoltaic properties if they are re-measured after a couple of days. One of the devices exhibiting this behavior is shown in Table 5.6. In the device sh44-1-f, improvement in Voc is seen. This might be because of Copper. If the devices are left for a couple of days after they are completely fabricated, Copper might diffuse into the shallow areas of the insulating layer making ZnSe a p-type contact to the absorber resulting in the improvement of Voc. It was also observed that the copper dots spread.

Devices showed better performance after spreading. There could be some chemical reaction taking place in the surface which might aid in improving the device parameters. The J-V response for the above device is shown in Fig 5.13(a) and (b).

Table 5.6 Effect of Time on Device Performance

Sample #	Voc (in V)	Voc (over time in V)	FF	Jsc(mA/cm ²)
sh44-1-f	0.140	0.270	31.7	5.42

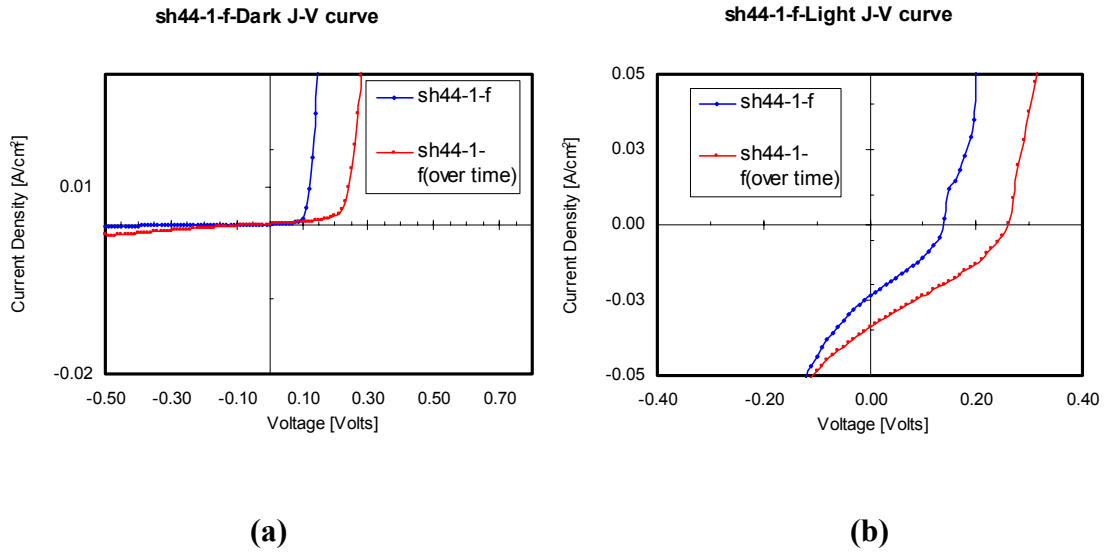


Fig 5.10(a) and (b) J-V Curve for Device # sh44-1-f

The initial measurements show that the series and shunt resistances in the dark are better. The later measurements showed a lot of shunting under illumination. Under illumination, there is no significant change in the series resistance. The spectral response of the device sh44-1-f measured after it is left over a period of time is shown in Fig 5.13.

sh44-1-f(7059/SnO₂:F-800 Å/CdSe-670 Å/580 Å/3 T He-14 min/ZnSe-200 Å/Cu-30 Å)

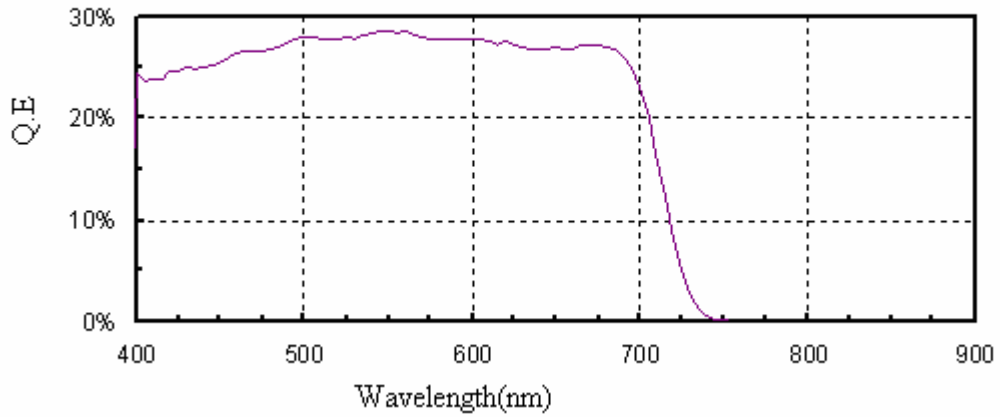


Fig 5.11 Spectral Response for Device # sh44-1-f

Q.E is less in the shorter wavelengths and it tends to rise as it reaches the mid wavelengths with the highest Q.E of approximately 28 % which is still a lesser value in comparison to the other devices.

Chapter 6

Conclusions

As discussed in the first chapter, the goal of achieving efficiencies greater than 25-30 % in a solar cell is possible only by fabricating a Tandem cell. A 4-terminal tandem solar cell has two cells of suitable band gaps placed one over the other with a proper encapsulant between them. According to the initial investigation, it was chosen that low band gap CIGS suits well as an absorber layer in the bottom cell. Significant efforts have been put in finding the suitable absorber for the top cell. In order to attain high efficiencies the band gap of the material should be between 1.5 eV and 2.0 eV. Few of the I-III-VI₂ compounds meet the requirement of having a band gap lying between 1.5 eV and 2.0 eV [30]. But these devices have not shown promising results. Further investigation resulted in opting for CdSe and Cd_{1-x}Zn_xTe as a choice of absorber layer in the top cell. The band gap of CdSe is 1.7 eV while Cd_{1-x}Zn_xTe has a tunable band gap.

As a part of this study, the possibility of using CdSe as an absorber layer in the top cell of the tandem solar cell has been investigated. The experiments performed partly confirmed the possible application of having CdSe as an attractive II-VI compound for solar cell applications. The various experiments performed showed that the absorber layer is deposited to suit the high temperature processing without causing any adverse effect to

the back contact. SnO_2 : F forms a good choice for the back contact with lower sheet resistance. Even after undergoing a subsequent high temperature processing during the deposition of CdSe, the sheet resistance values have not increased by a large magnitude. Hence SnO_2 : F is chosen as a back contact in standard CdSe solar cells.

The experimentation done has confirmed that n-type CdSe absorber layers have good electronic and structural properties. It was also observed that the deposition parameters like substrate temperature, source temperature, spacing, pressure in the reactor tube or the ambience largely determine the growth and the properties of CdSe films.

Ideally in a MIS structure, ZnSe should act as an insulating layer. It has good optical and physical properties which match with the absorber. Copper is deposited as a metal contact to ZnSe. There are some potential problems with this metal contact. Copper diffuses into deep regions near the junction and thereby shorting the devices. On the other hand it is suspected that deposition of an optimum amount of copper results in diffusion into the shallow regions of ZnSe and thereby forming a homogenous material Cu/ZnSe: Cu enhancing the device performance by making ZnSe p-type [29]. This behavior of Cu/ZnSe junction shows a deviation from MIS type devices. Therefore the amount of copper present is an important concern. Since it is a shiny metal, it has a high reflectivity and thereby losing some of the incident photons due to losses in reflection.

Hence the photo-currents generated are less. If copper can be replaced by a less reflective p- type metal contact to CdSe, then the chance of obtaining high photo-currents at the output is more.

Under standard deposition conditions, the thickness of the absorber layer is around 1.5 microns. It is desirable to have a completely depleted absorber so that most of the carriers generated within the diffusion length of the semiconductor can be collected before they recombine. In order to achieve a completely depleted absorber layer, the thickness of the absorber layer has to be decreased to 0.5 - 0.7 microns without adversely affecting the device output parameters. Further examination in obtaining a completely depleted absorber layer has to be achieved. Further experimentation has to be done to optimize the parameters and the thickness of the subsequent layers in achieving the same.

The Metal Insulating Semiconductor (MIS) structure can be replaced if we can dope the insulating layer to p-type and thereby forming a p-n junction between the window and the absorber layer. There should be minimum absorption loss in the layers above the absorber to enhance the device output parameters. A transparent front contact has to be deposited to replace copper and thereby we can overcome the losses at the front contact to a considerable extent.

In some cases, it was noticed that there is a variation in the device parameters from one device to the other device on the same substrate.

This might be due to the difference in the thickness of the different layers deposited. This issue has to be taken into consideration. In general, for the same conditions the devices showed good repeatability and reproducibility.

Most of the devices have generated reasonable V_{oc} 's and J_{sc} 's. The highest values achieved so far for V_{oc} and J_{sc} are 220 mV and 10.02 mA/cm². CdSe when deposited on CdS/SnO₂: F has resulted in a V_{oc} of around 350 mV, J_{sc} of 7.21 mA/cm² and a fill factor of 47.5 %.

References

- [1] D.Tarrant et al, "I-III-VI Multinary solar cells based on CuInSe₂", proceedings of the 23rd IEEE photovoltaic specialists conference, 372, (IEEE 1993).
- [2] M.Nishitani et al, "Photovoltaic properties of Cu (In, Ga)Se₂ thin film solar cell fabricated by coevaporation process", proceedings of the 24th IEEE photovoltaic specialists conference, 222, (IEEE 1994).
- [3] P.Mahawela, S.Jeedigunta, C.S.Ferekides and D.L.Morel, "Development of II-VI high bandgap devices for high efficiency tandem solar cells".
- [4] D.M.Chapin, C.S.Fuller and G.L.Pearson, "A new silicon p-n junction photo-cell for converting solar radiation into electrical power", J.Appl.Phys, 25,676(1954).
- [5] NREL Research photovoltaic research-"Creating electricity from an unlimited resource-sunlight".
- [6] National Renewable Energy Laboratories, "Photovoltaics program plan FY 1991-FY1995", National photovoltaics program, US Department of energy, Washington, DC (October 1999).
- [7] Adolf Goetberger et al, "Photovoltaic materials, history, status and outlook", August 2002.
- [8] M.A.Green, "Solar cells- operating principles, Technology and system application", Prentice Hall, Engle Wood Cliffs, NJ (1982).
- [9] S.M.Sze, "Physics of semiconductor devices", Wiley, New York (1981).
- [10] Stephen J.Fonash, "Solar cell device physics".
- [11] M.Russak, J.Eichman, H.Witzke, S.Deb and S.Chen, J.Electrochem.Soc:Solid-state science and technology, Vol 127,725(1980).
- [12] D.Bonnet and E.Rickus, Proceedings of the 14th IEEE PV Specialist Conference, 629(1980).

- [13] E Benmar, M.Rami, M.Fahoume, F.Chraibi, A.Ennaoui," Electrodeposited cadmium Selenide films for solar cells", *Ann.Chim.Sci.Mat*, 1998, 23, pp.369-372.
- [14] Chouhaid Nasr, Prashant V.Kamat, Surat Hotchandani," Photo-electrochemical behavior of couples SnO₂/CdSe nano crystalline semiconductor films", *Journal of Electroanalytical Chemistry* 420(1997)201-207.
- [15] Meera Ramrakhiani," Zinc doped polycrystalline CdSe film for solar energy conversion", *Material Science and Engineering B35* (1995)493-496.
- [16] Cristian Baban, G.I.Rusu," On the structural and optical characteristics of CdSe thin films", *Applied Surface Science* (p 6-12).
- [17] D.Pahinettam Padiyan^{a,*}, A.Marikani^b, K.R.murali^c,"Influence of thickness and substrate temperature on electrical and photoelectrical properties of vacuum deposited CdSe thin films", *Materials Chemistry and Physics* 78(2002)51-58.
- [18] C.Sene, H.Nguyen cong, M.Dieng, P.Chartier,"Hybrid photovoltaic structures based on polymer/Chemically grown Cadmium Selenide films: Effect of Silicongtungstic acid on the junction properties", *Materials Research Bulletin* 35 (2000)1541-1553.
- [19] S.S.Kale, C.D.Lokhande,"Thickness dependent properties of chemically deposited CdSe thin films", *Materials Chemistry and Physics* 62(2000)103-108.
- [20] R.M.Abdel-latif," Direct current conductivity of evaporated Cadmium Selenide films", *Physica B* 270(1999) 366-370.
- [21] V.Nadenau, D.Hariskos and H.W.Schock, proceedings of 14th European Photovoltaic solar energy conference, Stephens and Assoc, Bedford, U.K., 1997 p.1250.
- [22] P.Gashin, A.Focsha, T.Potlog, A.Simashkevich and V.Leondar,"Solar Energy Materials and Solar cells", 46, 323, (1997).
- [23] A.VanCalster, F.Vanfleteren, I.DeRycke, J.De Baets, *J.Appl.Phys.* 64 (1988)3282.
- [24] N.G.Patel, C.J.Panchal, K.K Makhijja, *Cryst.Res.Technol.* 29 (1994)1013.
- [25] V.A.Smyntyana, V.Gerasutenko, S.Kashulis, G.Mattogno, S.Reghini, *Sensors Actuators* 19(1994)464.
- [26] B.Bonello, B.Fernandez, *J.Phys.Chem.Solids* 54(1993)209.
- [27] J.C.Schottmiller, R.W.Francis, C.Wood, US patent 3884688, 1975.
- [28] B.J.Curtis, H.Kiess, H.R.Brunner, K.Frick, *Photogr.Sci.Eng.* 24 (1980)244.

[29] P.Mahawela, S.Jeedigunta, C.S.Ferekides and D.L.Morel,"Analysis of carrier transport phenomena in high band gap II-VI based MIS photovoltaic devices".

[30] D.Braunger,Th.Durr,D.Hariskos,Ch.Koble,Th.Walter,N.Wieser and H.W.Schock,"Improved Voc in CuInSe₂-based Solar Cells", Proceedings of the 25th IEEE PVSC, Washington, D.C.,1996,p.1001.